

Figures 1 e 2 on Page 19.

Chief Editor
Carlos Rochitte

Internacional Coeditor
João Lima

Editors
Alexandre Colafranceschi
Gláucia Moraes
Ieda Jatene
João Cavalcante
Marcio Bittencourt
Marina Okoshi
Mauricio Scanavacca
Paulo Jardim
Pedro Lemos
Ricardo Stein
Ruhong Jiang
Tiago Senra
Vitor Guerra

Transient left anterior fascicular block

Myocardial involvement in Sweet Syndrome

Left Bundle Branch Block

An Unusual Pacemaker-Induced Tachycardia

SCAD in a patient with CTX

Prolonged pleural effusion after Fontan operation in complex heart defect

Corrected transposition of the great arteries, with good natural evolution until 65 years

Contents

Case Report

Transient Prominent Anterior QRS Forces in Acute Left Main Coronary Artery Subocclusion: Transient Left Septal Fascicular Block

Andrés Ricardo Pérez-Riera, Raimundo Barbosa-Barros, Rodrigo Daminello Raimundo, Luiz Carlos de Abreu, Marcos Célio de Almeida, Kjell Nikus

.....page 1

Myocardial Involvement in Sweet Syndrome: A Rare Finding in a Rare Condition

Luís Graça-Santos, Katarina Kieselova, Fernando Montenegro-Sá, Joana Guardado, João Morais

.....page 6

Idiopathic Left-Bundle Branch Block and Unexplained Symptom At Exercise: A Case Report

Guilherme Veiga Guimarães e Edimar Alcides Bocchi

.....page 10

An Unusual Pacemaker-Induced Tachycardia

Madalena Coutinho-Cruz, Guilherme Portugal, Pedro Silva-Cunha, Mário Martins-Oliveira

.....page 14

Spontaneous Coronary Artery Dissection in a patient with Cerebrotendinous Xanthomatosis

Maria Júlia Silveira Souto, Marcos Antônio Almeida-Santos, Eduardo José Pereira Ferreira, Luiz Flávio Galvão Gonçalves, Joselina Luzia Menezes Oliveira, Antônio Carlos Sobral Sousa

.....page 18

A Case of Acute Myocardial Infarction and Pericarditis Unmasking Metastatic Involvement of the Heart

Sofia Torres, Mariana Vasconcelos, Carla Sousa, Antonio J. Madureira, Alzira Nunes, Maria Júlia Maciel

.....page 22

A Complicated "One Segment" Myocardial Infarction: The Role of Cardiovascular Imaging

Ana Rita Pereira, Ana Rita Almeida, Inês Cruz, Luis Rocha Lopes, Maria José Loureiro, Hélder Pereira

.....page 25

Clinicoradiological Session

Case 4/2020 – Prolonged Time (38 Days) of Bilateral Pleural Effusion after Cavopulmonary Surgery, Relieved by Embolization of Systemic-Pulmonary Collateral Vessels, in a 40-Month-Old Child with Complex Heart Disease

Edmar Atik, Raul Arrieta, Fernando Antibas Atik

.....page 31

Case 5/2020 – Corrected Transposition of the Great Arteries, with Good Natural Evolution in a 65-Year-Old Woman

Edmar Atik, Renato Maluf Auge, Alessandra Costa Barreto, Maria Angélica Binotto

.....page 34

Case 6/2020 – 16-Year-Old Adolescent with Severe Pulmonary Stenosis At Valvar Level, After Correction of *Truncus Arteriosus* using the Barbero-Marcial Technique in the First Month of Life

Edmar Atik e Miguel Barbero-Marcial

.....page 37



ABC Cardiol

Arquivos Brasileiros de Cardiologia

JOURNAL OF BRAZILIAN SOCIETY OF CARDIOLOGY - Published since 1943

Scientific Director

Fernando Bacal

Chief Editor

Carlos Eduardo Rochitte

International Co-editor

João Lima

Social Media Editor

Tiago Senra

Chinese Consulting Editor

Ruhong Jiang

Associated Editors

Clinical Cardiology

Gláucia Maria Moraes
de Oliveira

Surgical Cardiology

Alexandre Siciliano
Colafranceschi

Interventionist Cardiology

Pedro A. Lemos

Pediatric/Congenital

Cardiology

Ieda Biscegli Jatene

Vitor C. Guerra

Arrhythmias/Pacemaker

Mauricio Scanavacca

Non-Invasive Diagnostic Methods

João Luiz Cavalcante

Basic or Experimental Research

Marina Politi Okoshi

Epidemiology/Statistics

Marcio Sommer Bittencourt

Arterial Hypertension

Paulo Cesar B. V. Jardim

Ergometrics, Exercise and Cardiac Rehabilitation

Ricardo Stein

First Editor (1948-1953)

† Jairo Ramos

Editorial Board

Brazil

Aguinaldo Figueiredo de Freitas Junior – Universidade Federal de Goiás (UFG),
Goiânia GO – Brazil

Alfredo José Mansur – Faculdade de Medicina da Universidade de São Paulo
(FMUSP), São Paulo, SP – Brazil

Aloir Queiroz de Araújo Sobrinho – Instituto de Cardiologia do Espírito Santo,
Vitória, ES – Brazil

Amanda Guerra de Moraes Rego Sousa – Instituto Dante Pazzanese de
Cardiologia/Fundação Adib Jatene (IDPC/FAJ), São Paulo, SP – Brazil

Ana Clara Tude Rodrigues – Hospital das Clínicas da Universidade de São Paulo
(HCFMUSP), São Paulo, SP – Brazil

André Labrunie – Hospital do Coração de Londrina (HCL), Londrina, PR – Brazil

Andrei Carvalho Sposito – Universidade Estadual de Campinas (UNICAMP),
Campinas, SP – Brazil

Angelo Amato Vincenzo de Paola – Universidade Federal de São Paulo
(UNIFESP), São Paulo, SP – Brazil

Antonio Augusto Barbosa Lopes – Instituto do Coração InCor Hc Fmusp
(INCOR), São Paulo, SP – Brazil

Antonio Carlos de Camargo Carvalho – Universidade Federal de São Paulo
(UNIFESP), São Paulo, SP – Brazil

Antônio Carlos Palandri Chagas – Universidade de São Paulo (USP), São Paulo,
SP – Brazil

Antonio Carlos Pereira Barretto – Universidade de São Paulo (USP), São Paulo,
SP – Brazil

Antonio Cláudio Lucas da Nóbrega – Universidade Federal Fluminense (UFF),
Rio de Janeiro, RJ – Brazil

Antonio de Padua Mansur – Faculdade de Medicina da Universidade de São
Paulo (FMUSP), São Paulo, SP – Brazil

Ari Timerman (SP) – Instituto Dante Pazzanese de Cardiologia (IDPC), São
Paulo, SP – Brazil

Armênio Costa Guimarães – Liga Bahiana de Hipertensão e Aterosclerose,
Salvador, BA – Brazil

Ayrton Pires Brandão – Universidade do Estado do Rio de Janeiro (UERJ), Rio
de Janeiro, RJ – Brazil

Beatriz Matsubara – Universidade Estadual Paulista Júlio de Mesquita Filho
(UNESP), São Paulo, SP – Brazil

Brivaldo Markman Filho – Universidade Federal de Pernambuco (UFPE), Recife,
PE – Brazil

Bruno Caramelli – Universidade de São Paulo (USP), São Paulo, SP – Brazil

Carisi A. Polanczyk – Universidade Federal do Rio Grande do Sul (UFRGS),
Porto Alegre, RS – Brazil

Carlos Eduardo Rochitte – Instituto do Coração do Hospital das Clínicas da
Faculdade de Medicina (INCOR HCFMUSP), São Paulo, SP – Brazil

Carlos Eduardo Suaide Silva – Universidade de São Paulo (USP), São Paulo,
SP – Brazil

Carlos Vicente Serrano Júnior – Instituto do Coração (InCor HCFMUSP), São
Paulo, SP – Brazil

Celso Amodeo – Instituto Dante Pazzanese de Cardiologia/Fundação Adib
Jatene (IDPC/FAJ), São Paulo, SP – Brazil

Charles Mady – Universidade de São Paulo (USP), São Paulo, SP – Brazil

Claudio Gil Soares de Araujo – Universidade Federal do Rio de Janeiro (UFRJ),
Rio de Janeiro, RJ – Brazil

Cláudio Tinoco Mesquita – Universidade Federal Fluminense (UFF), Rio de
Janeiro, RJ – Brazil

Cleonice Carvalho C. Mota – Universidade Federal de Minas Gerais (UFMG),
Belo Horizonte, MG – Brazil

Clerio Francisco de Azevedo Filho – Universidade do Estado do Rio de Janeiro
(UERJ), Rio de Janeiro, RJ – Brazil

Dalton Bertolim Prêcoma – Pontifícia Universidade Católica do Paraná (PUC/
PR), Curitiba, PR – Brazil

Dário C. Sobral Filho – Universidade de Pernambuco (UPE), Recife, PE – Brazil

Décio Mion Junior – Hospital das Clínicas da Faculdade de Medicina da
Universidade de São Paulo (HCFMUSP), São Paulo, SP – Brazil

Denilson Campos de Albuquerque – Universidade do Estado do Rio de Janeiro
(UERJ), Rio de Janeiro, RJ – Brazil

Djair Brindeiro Filho – Universidade Federal de Pernambuco (UFPE), Recife,
PE – Brazil

Domingo M. Brailo – Universidade Estadual de Campinas (UNICAMP), São
Paulo, SP – Brazil

Edmar Atik – Hospital Sírio Libanês (HSL), São Paulo, SP – Brazil

Emilio Hideyuki Moriguchi – Universidade Federal do Rio Grande do Sul
(UFRGS) Porto Alegre, RS – Brazil

Enio Buffolo – Universidade Federal de São Paulo (UNIFESP), São Paulo, SP – Brazil

Eulógio E. Martinez Filho – Instituto do Coração (InCor), São Paulo, SP – Brazil

Evandro Tinoco Mesquita – Universidade Federal Fluminense (UFF), Rio de
Janeiro, RJ – Brazil

Expedito E. Ribeiro da Silva – Universidade de São Paulo (USP), São Paulo,
SP – Brazil

Fábio Vilas Boas Pinto – Secretaria Estadual da Saúde da Bahia (SESAB),
Salvador, BA – Brazil

Fernando Bacal – Universidade de São Paulo (USP), São Paulo, SP – Brazil

Flávio D. Fuchs – Universidade Federal do Rio Grande do Sul (UFRGS), Porto Alegre, RS – Brazil

Francisco Antonio Helfenstein Fonseca – Universidade Federal de São Paulo (UNIFESP), São Paulo, SP – Brazil

Cilson Soares Feitosa – Escola Bahiana de Medicina e Saúde Pública (EBMSP), Salvador, BA – Brazil

Glaucia Maria M. de Oliveira – Universidade Federal do Rio de Janeiro (UFRJ), Rio de Janeiro, RJ – Brazil

Hans Fernando R. Dohmann, AMIL – ASSIST. MEDICA INTERNACIONAL LTDA., Rio de Janeiro, RJ – Brazil

Humberto Villacorta Junior – Universidade Federal Fluminense (UFF), Rio de Janeiro, RJ – Brazil

Ines Lessa – Universidade Federal da Bahia (UFBA), Salvador, BA – Brazil

Iran Castro – Instituto de Cardiologia do Rio Grande do Sul (IC/FUC), Porto Alegre, RS – Brazil

Jarbas Jakson Dinkhuysen – Instituto Dante Pazzanese de Cardiologia/Fundação Adib Jatene (IDPC/FAJ), São Paulo, SP – Brazil

João Pimenta – Instituto de Assistência Médica ao Servidor Público Estadual (IAMSPE), São Paulo, SP – Brazil

Jorge Ilha Guimarães – Fundação Universitária de Cardiologia (IC FUC), Porto Alegre, RS – Brazil

José Antonio Franchini Ramires – Instituto do Coração InCor Hc Fmusp (INCOR), São Paulo, SP – Brazil

José Augusto Soares Barreto Filho – Universidade Federal de Sergipe, Aracaju, SE – Brazil

José Carlos Nicolau – Instituto do Coração (InCor), São Paulo, SP – Brazil

José Lázaro de Andrade – Hospital Sírio Libanês, São Paulo, SP – Brazil

José Péricles Esteves – Hospital Português, Salvador, BA – Brazil

Leonardo A. M. Zornoff – Faculdade de Medicina de Botucatu Universidade Estadual Paulista Júlio de Mesquita Filho (UNESP), Botucatu, SP – Brazil

Leopoldo Soares Piegas – Instituto Dante Pazzanese de Cardiologia/Fundação Adib Jatene (IDPC/FAJ) São Paulo, SP – Brazil

Lucia Campos Pellanda – Fundação Universidade Federal de Ciências da Saúde de Porto Alegre (UFCSPA), Porto Alegre, RS – Brazil

Luís Eduardo Paim Rohde – Universidade Federal do Rio Grande do Sul (UFRGS), Porto Alegre, RS – Brazil

Luís Cláudio Lemos Correia – Escola Bahiana de Medicina e Saúde Pública (EBMSP), Salvador, BA – Brazil

Luiz A. Machado César – Fundação Universidade Regional de Blumenau (FURB), Blumenau, SC – Brazil

Luiz Alberto Piva e Mattos – Instituto Dante Pazzanese de Cardiologia (IDPC), São Paulo, SP – Brazil

Marcia Melo Barbosa – Hospital Socor, Belo Horizonte, MG – Brazil

Marcus Vinícius Bolívar Malachias – Faculdade Ciências Médicas MG (FCMMG), Belo Horizonte, MG – Brazil

Maria da Consolação V. Moreira – Universidade Federal de Minas Gerais (UFMG), Belo Horizonte, MG – Brazil

Mario S. S. de Azeredo Coutinho – Universidade Federal de Santa Catarina (UFSC), Florianópolis, SC – Brazil

Maurício Ibrahim Scanavacca – Universidade de São Paulo (USP), São Paulo, SP – Brazil

Max Grinberg – Instituto do Coração do Hcfmusp (INCOR), São Paulo, SP – Brazil

Michel Batlouni – Instituto Dante Pazzanese de Cardiologia (IDPC), São Paulo, SP – Brazil

Murilo Foppa – Hospital de Clínicas de Porto Alegre (HCPA), Porto Alegre, RS – Brazil

Nadine O. Clausell – Universidade Federal do Rio Grande do Sul (UFRGS), Porto Alegre, RS – Brazil

Orlando Campos Filho – Universidade Federal de São Paulo (UNIFESP), São Paulo, SP – Brazil

Otávio Rizzi Coelho – Universidade Estadual de Campinas (UNICAMP), Campinas, SP – Brazil

Otoni Moreira Gomes – Universidade Federal de Minas Gerais (UFMG), Belo Horizonte, MG – Brazil

Paulo Andrade Lotufo – Universidade de São Paulo (USP), São Paulo, SP – Brazil

Paulo Cesar B. V. Jardim – Universidade Federal de Goiás (UFG), Brasília, DF – Brazil

Paulo J. F. Tucci – Universidade Federal de São Paulo (UNIFESP), São Paulo, SP – Brazil

Paulo R. A. Caramori – Pontifícia Universidade Católica do Rio Grande do Sul (PUCRS), Porto Alegre, RS – Brazil

Paulo Roberto B. Évora – Universidade de São Paulo (USP), São Paulo, SP – Brazil

Paulo Roberto S. Brofman – Instituto Carlos Chagas (FIOCRUZ/PR), Curitiba, PR – Brazil

Pedro A. Lemos – Hospital das Clínicas da Faculdade de Medicina da USP (HCFMUSP), São Paulo, SP – Brazil

Protásio Lemos da Luz – Instituto do Coração do Hcfmusp (INCOR), São Paulo, SP – Brazil

Reinaldo B. Bestetti – Universidade de Ribeirão Preto (UNAERP), Ribeirão Preto, SP – Brazil

Renato A. K. Kalil – Instituto de Cardiologia do Rio Grande do Sul (IC/FUC), Porto Alegre, RS – Brazil

Ricardo Stein – Universidade Federal do Rio Grande do Sul (UFRS), Porto Alegre, RS – Brazil

Salvador Rassi – Faculdade de Medicina da Universidade Federal de Goiás (FM/GO), Goiânia, GO – Brazil

Sandra da Silva Mattos – Real Hospital Português de Beneficência em Pernambuco, Recife, PE – Brazil

Sandra Fuchs – Universidade Federal do Rio Grande do Sul (UFRGS), Porto Alegre, RS – Brazil

Sergio Timerman – Hospital das Clínicas da Faculdade de Medicina da USP (INCOR HC FMUSP), São Paulo, SP – Brazil

Silvio Henrique Barberato – Cardioeco Centro de Diagnóstico Cardiovascular (CARDIOECO), Curitiba, PR – Brazil

Tales de Carvalho – Universidade do Estado de Santa Catarina (UDESC), Florianópolis, SC – Brazil

Vera D. Aiello – Instituto do Coração do Hospital das Clínicas da (FMUSP, INCOR), São Paulo, SP – Brazil

Walter José Gomes – Universidade Federal de São Paulo (UNIFESP), São Paulo, SP – Brazil

Weimar K. S. B. de Souza – Faculdade de Medicina da Universidade Federal de Goiás (FMUFG), Goiânia, GO – Brazil

William Azem Chalela – Instituto do Coração (INCOR HCFMUSP), São Paulo, SP – Brazil

Wilson Mathias Junior – Instituto do Coração (InCor) do Hospital das Clínicas da Faculdade de Medicina da Universidade de São Paulo (HCFMUSP), São Paulo, SP – Brazil

Exterior

Adelino F. Leite-Moreira – Universidade do Porto, Porto – Portugal

Alan Maisel – Long Island University, Nova York – USA

Aldo P. Maggioni – ANMCO Research Center, Florença – Italy

Ana Isabel Venâncio Oliveira Galrinho – Hospital Santa Marta, Lisboa – Portugal

Ana Maria Ferreira Neves Abreu – Hospital Santa Marta, Lisboa – Portugal

Ana Teresa Timóteo – Hospital Santa Marta, Lisboa – Portugal

Cândida Fonseca – Universidade Nova de Lisboa, Lisboa – Portugal

Fausto Pinto – Universidade de Lisboa, Lisboa – Portugal

Hugo Grancelli – Instituto de Cardiología del Hospital Español de Buenos Aires – Argentina

James de Lemos – Parkland Memorial Hospital, Texas – USA

João A. Lima, Johns – Johns Hopkins Hospital, Baltimore – USA

John G. F. Cleland – Imperial College London, Londres – England

Jorge Ferreira – Hospital de Santa Cruz, Carnaxide – Portugal

Manuel de Jesus Antunes – Centro Hospitalar de Coimbra, Coimbra – Portugal

Marco Alves da Costa – Centro Hospitalar de Coimbra, Coimbra – Portugal

Maria João Soares Vidigal Teixeira Ferreira – Universidade de Coimbra, Coimbra – Portugal

Maria Pilar Tornos – Hospital Quirónsalud Barcelona, Barcelona – Spain

Nuno Bettencourt – Universidade do Porto, Porto – Portugal

Pedro Brugada – Universiteit Brussel, Brussels – Belgium

Peter A. McCullough – Baylor Heart and Vascular Institute, Texas – USA

Peter Libby – Brigham and Women's Hospital, Boston – USA

Piero Anversa – University of Parma, Parma – Italy

Roberto José Palma dos Reis – Hospital Polido Valente, Lisboa – Portugal

Sociedade Brasileira de Cardiologia

President

Marcelo Antônio Cartaxo Queiroga Lopes

Vice President

Celso Amodeo

Financial Director

Ricardo Mourilhe Rocha

Scientific Director

Fernando Bacal

Managing Director

Olga Ferreira de Souza

Service Quality Director

Sílvio Henrique Barberato

Communication Director

Harry Corrêa Filho

Information Technology Director

Leandro Ioschpe Zimmerman

Governmental Relations Director

Nasser Sarkis Simão

State and Regional Relations Director

João David de Souza Neto

Cardiovascular Health Promotion Director – SBC/Funcor

José Francisco Kerr Saraiva

Director of Specialized Departments

Andréa Araujo Brandão

Research Director

David de Pádua Brasil

Coordinator of Science, Technology and Innovation

Ludhmila Abrahão Hajjar

Coordinator of Continued Medical Education

Brivaldo Markman Filho

Coordinator of Management Supervision and Internal Control

Gláucia Maria Moraes de Oliveira

Coordinator of Compliance and Transparency

Marcelo Matos Cascudo

Coordinator of Strategic Affairs

Hélio Roque Figueira

Editor-in-Chief of the Arquivos Brasileiros de Cardiologia

Carlos Eduardo Rochitte

Editor-in-Chief of the IJCS

Claudio Tinoco Mesquita

Coordinator of the University of the Heart

Evandro Tinoco Mesquita

Coordinator of Standards and Guidelines

Paulo Ricardo Avancini Caramori

Presidents of State and Regional Brazilian Societies of Cardiology:

SBC/AL – Carlos Romerio Costa Ferro

SBC/AM – Kátia do Nascimento Couceiro

SBC/BA – Gilson Soares Feitosa Filho

SBC/CE – Gentil Barreira de Aguiar Filho

SBC/DF – Alexandra Oliveira de Mesquita

SBC/ES – Tatiane Mascarenhas Santiago Emerich

SBC/GO – Leonardo Sara da Silva

SBC/MA – Mauro José Mello Fonseca

SBC/MG – Henrique Patrus Mundim Pena

SBC/MS – Gabriel Doreto Rodrigues

SBC/MT – Marcos de Thadeu Tenuta Junior

SBC/NNE – Nivaldo Menezes Filgueiras Filho

SBC/PA – Dilma do Socorro Moraes de Souza

SBC/PB – Lenine Angelo Alves Silva

SBC/PE – Fernando Ribeiro de Moraes Neto

SBC/PI – Luiz Bezerra Neto

SBC/PR – Raul DAurea Mora Junior

SOCERJ – Wolney de Andrade Martins

SBC/RN – Maria Sanali Moura de Oliveira Paiva

SOCERON – Daniel Ferreira Mugrabi

SOCERGS – Mario Wiehe

SBC/SC – Amberson Vieira de Assis

SBC/SE – Eryca Vanessa Santos de Jesus

SOCESP – João Fernando Monteiro Ferreira

Presidents of the Specialized Departments and Study Groups

SBC/DA – Antonio Carlos Palandri Chagas

SBC/DCC – Bruno Caramelli

SBC/DCC/CP – Klebia Magalhães Pereira
Castello Branco

SBC/DCM – Celi Marques Santos

SBC/DECAGE – Izo Helber

SBC/DEIC – Evandro Tinoco Mesquita

SBC/DERC – Gabriel Leo Blacher Grossman

SBC/DFCVR – Antoinette Oliveira Blackman

SBC/DHA – Audes Diógenes de
Magalhães Feitosa

SBC/DIC – Carlos Eduardo Rochitte

SBCCV – Eduardo Augusto Victor Rocha

SOBRAC – Ricardo Alkmim Teixeira

SBHCI – Ricardo Alves da Costa

DCC/GAPO – Danielle Menosi Gualandro

DCC/GECETI – Luiz Bezerra Neto

DCC/GECO – Roberto Kalil Filho

DCC/GEMCA – Roberto Esporcatté

DCC/GERTC – Adriano Camargo de
Castro Carneiro

DEIC/GEICPED – Estela Azeka

DEIC/GEMIC – Marcus Vinicius Simões

DERC/GECESP – Clea Simone Sabino de
Souza Colombo

DERC/GEEN – Lara Cristiane Terra
Ferreira Carreira

DERC/GERCPM – Carlos Alberto
Cordeiro Hossri

GECIP – Marcelo Luiz da Silva Bandeira

GEECG – Carlos Alberto Pastore

DCC/GETA – Carlos Vicente Serrano Junior

DCC/GECRA – Sandra Marques e Silva

Arquivos Brasileiros de Cardiologia

Volume 115, Nº 1, Suppl. 1, July 2020

Indexing: ISI (Thomson Scientific), Cumulated Index Medicus (NLM), SCOPUS, MEDLINE, EMBASE, LILACS, SciELO, PubMed



Address: Av. Marechal Câmara, 160 - 3º andar - Sala 330
20020-907 • Centro • Rio de Janeiro, RJ • Brasil

Phone.: (21) 3478-2700

E-mail: arquivos@cardiol.br

www.arquivosonline.com.br

SciELO: www.scielo.br

Commercial Department

Phone: (11) 3411-5500

E-mail: comerciaisp@cardiol.br

Editorial Production

SBC - Internal Publication Department

Graphic Design and Diagramming

SBC - Internal Design Department

The ads showed in this issue are of the sole responsibility of advertisers, as well as the concepts expressed in signed articles are of the sole responsibility of their authors and do not necessarily reflect the views of SBC.

This material is for exclusive distribution to the medical profession. The Brazilian Archives of Cardiology are not responsible for unauthorized access to its contents and that is not in agreement with the determination in compliance with the Collegiate Board Resolution (DRC) N. 96/08 of the National Sanitary Surveillance Agency (ANVISA), which updates the technical regulation on Drug Publicity, Advertising, Promotion and Information. According to Article 27 of the insignia, "the advertisement or publicity of prescription drugs should be restricted solely and exclusively to health professionals qualified to prescribe or dispense such products (...)".

To ensure universal access, the scientific content of the journal is still available for full and free access to all interested parties at:
www.arquivosonline.com.br.



Affiliated at the Brazilian
Medical Association

SUPPORT




Ministério da
Educação

Ministério da
Ciência e Tecnologia



Transient Prominent Anterior QRS Forces in Acute Left Main Coronary Artery Subocclusion: Transient Left Septal Fascicular Block

Andrés Ricardo Pérez-Riera,¹  Raimundo Barbosa-Barros,² Rodrigo Daminello Raimundo,¹ Luiz Carlos de Abreu,¹ Marcos Célio de Almeida,³ Kjell Nikus⁴

Centro Universitario Saúde ABC,¹ Santo André, SP - Brazil

Hospital de Messejana Dr. Carlos Alberto Studart Gomes,² Fortaleza, CE - Brazil

Universidade de Brasília - Instituto de Biologia-Genética e Morfologia,³ Brasília, DF - Brazil

Heart Center, Tampere University Hospital and Faculty of Medicine and Life Sciences,⁴ Tampere - Finland

Introduction

The left main coronary artery (LMCA) originates from the left sinus of Valsalva, passes between the main pulmonary artery and the left atrial appendage before entering the coronary sulcus and bifurcates into the left anterior descending (LAD) and the left circumflex (LCX) coronary arteries. In most individuals, the LMCA supplies $\approx 75\%$ of the left ventricle (LV).¹ Significant stenosis, which may lead to stable angina and/or acute coronary syndrome, places the patient at risk of life-threatening acute left ventricular failure and malignant arrhythmias. Patient prognosis of LMCA disease can be improved with coronary artery bypass grafting (CABG). With technical improvement and effective anti-thrombotic medication, percutaneous coronary intervention (PCI) has evolved as an alternative therapeutic modality. In patients with severe LMCA disease having low to intermediate anatomic complexity, both CABG and PCI are effective methods of revascularization with comparable long-term rates of death, myocardial infarction, and stroke.² Patients most suitable for LMCA stenting are those with isolated ostial/mid LMCA disease, protected LMCA disease and those who undergo an elective stenting procedure. In a recent study, 8% mortality and 8% target lesion revascularization rate during one-year follow-up was reported.³

Case description

A 72-year-old Caucasian male presented at the emergency department complaining of prolonged oppressive chest pain at rest since ≈ 1 hour associated with cold diaphoresis and respiratory distress. He had a history of type 2 diabetes mellitus and dyslipidemia had been detected four years before. Two months earlier, he had oppressive precordial pain on moderate exertion, which disappeared rapidly after rest. Figure 1 shows

the ECG at admission and Figure 2-A an ECG performed 30 days before. The coronary angiography indicated subocclusion (91-99% diameter stenosis) in the middle portion of the LMCA (Figure 2-B). CABG was immediately proposed, but the patient refused. He successfully underwent PCI with DES implantation without in-hospital complications. During the 6-month follow-up no target lesion revascularization was required on the LMCA. The patient remained asymptomatic even at efforts and several follow-up ECGs were normal.

Discussion

An ECG performed due to stable angina symptoms 30 days before the hospital admission, showed a pattern suggestive of LMCA disease and possibly some degree of LSFB.^{4,5} These “minimal findings” in the scenario of stable angina should alert the clinician about the possibility of severe myocardial ischemia in patients without a logical explanation for the ECG findings, such as left ventricular hypertrophy with strain in structural heart disease. Both ECG features are evident, with more pronounced ischemic findings in the ECG performed at admission when the patient had acute coronary syndrome.

Several successive manuscripts from our group and others have shown that a large proportion of cases with transient left septal fascicular block (LSFB), manifested by prominent anterior QRS forces, is caused by critical proximal obstruction of the LAD before its first septal perforator branch.⁶⁻⁹ As the LAD is a continuation of the LMCA, significant LMCA obstruction, may lead to ischemia in the mid-portion and apical territory of the left ventricle, where the left septal fascicle runs, thereby causing LSFB.

In the presence of LSFB, the sequence of ventricular activation begins only at two points:

The base of the anterolateral papillary muscle (ALPM) of the mitral valve dependent on the left anterior fascicle (LAF) in the anterior paraseptal wall, just below the ALPM attachment (1_{AM} vector);

The base of the posteromedial papillary muscle of the mitral valve (PMPM) dependent on the left posterior fascicle (LPF). It is located in the posterior paraseptal wall, at about one-third of the distance from the apex to the base (posteroinferior vector -1_{PI}). These two initial vectors have opposite directions, and they cancel each other with minimal predominance of the 1_{PI} vector directed backward (Figure 3). This explains the absence of the normal initial convexity to the right of the QRS loop in the horizontal plane, dependent on the 1_{AM} septal vector (or

Keywords

Coronary Occlusion; Truncus Arterious; Acute Coronary Syndrome; Fibrinolytic Agents; Percutaneous Coronary Intervention; Angina, Stable; Electrocardiography/methods.

Mailing Address: Andrés Ricardo Pérez-Riera •

Rua Nicolau Barreto, 258. Postal Code 04583-000, São Paulo, SP - Brazil

E-mail: riera@uol.com.br, arperezriera@gmail.com

Manuscript received November 18, 2018, revised manuscript May 30, 2019, accepted August 18, 2019

DOI: <https://doi.org/10.36660/abc.20180363>

Case Report

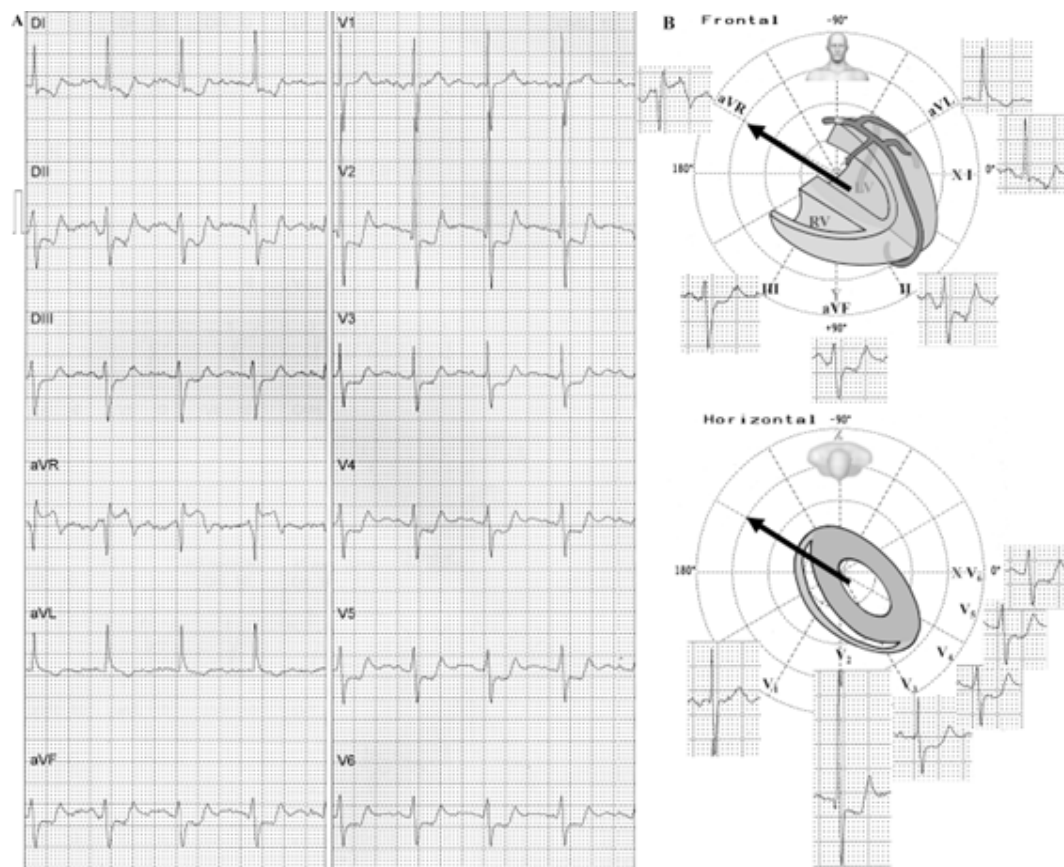


Figure 1 – ECG at admission (A) and the injury vector in the frontal and horizontal planes (B). A) Widespread ST-segment depression in I, II, III (II>III) and VF and from V2 to V6 waves. Diffuse ST-segment depression in the inferolateral leads (≥ 7 leads with ST-depression) and reciprocal ST-segment elevation in the aVR lead. In addition, atypical left anterior fascicular block (LAFB), QRS axis -40° , SII>SII, and absence of initial q wave in I and aVL by absence of the first left middle septal vector (in typical LAFB the first 10-20 ms vectors are directed to $+120^\circ$).⁴ B) Frontal plane (FP): The ST injury vector (arrow) is directed upward and rightward pointing towards the aVR lead (-150°). When this vector is located between -90° and $\pm 180^\circ$ in the FP, it is indicative of LMCA obstruction in up to 100% of cases;⁵ ST-segment depression in the inferior leads with STII>STIII; Horizontal plane: the ST injury vector is directed to the right and leftward (arrow), perpendicular to V1. ST segment depression from V2 to V6.

Penaloza-Tranchesi vector).¹⁰ Next, the stimulus is directed to the mid-septal or left paraseptal region, blocked by numerous Purkinje passage areas, thus shifting the forces to the front and the left, resulting in prominent anterior forces (PAF). Figure 4 shows two cases where the trifascicular anatomy of the left His system is evident. Ironically, both cases come from the school of electrocardiography that coined the bifascicular concept of the left His system.¹¹

Left fascicles blood supply

LAF: the blood supply to the LAF of the LBB originated in 50 % of the cases not only from the anterior septal branch of the LAD, but also from the atrioventricular (AV) nodal artery, a branch of the right coronary artery (RCA) in 90 % of the cases and of the LCX in 10%.¹² Thus, anatomic data support the observation that occlusion of the proximal segment of the LAD is not a prerequisite for the occurrence of LAFB. The appearance of LAFB during acute myocardial infarction

is not a sign of a coexistent significant stenosis of the LAD or of more severe or extensive coronary artery disease. In these patients, other mechanisms such as the degree of the coronary collateral circulation may play a role in the occurrence of this conduction disturbance and supports the experimental and clinical reports that LAFB may be due to lesions involving the His bundle by means of a longitudinal dissociation of this structure.¹³

LPF: the broad nature of the LPF, its protected location in the left ventricular inflow tract, as well as its dual blood supply¹⁴ makes isolated LPFB very rare.¹⁵ The PMPM where LPF ends is supplied by arterial branches that terminate on the diaphragmatic surface of the LV, and most commonly by a junction of terminal branches of the LCX and of the RCA. When the LCX supplies nearly all the diaphragmatic surface of the LV (10 % of human hearts), its branches provide the entire blood supply for the PMPM. The LPF is irrigated in 10% of cases by LAD only, in 40% of cases by LAD and RCA and in 50% of cases by RCA only.

Case Report

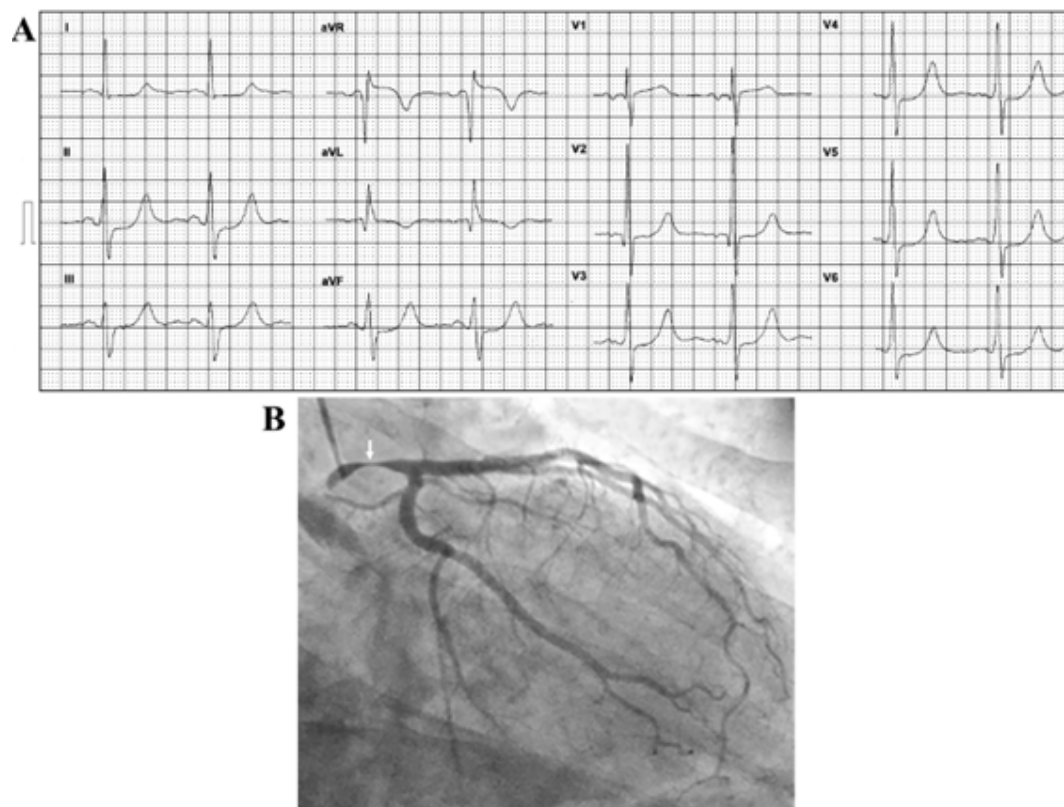


Figure 2 – A) ECG performed 30 days before: left atrial enlargement, prominent anterior QRS forces in V2 with qRs pattern in V1-V2, R wave voltage in V2 >15 mm (23 mm), prolonged R-wave peak time in right precordial leads (≥ 35 ms), ST-segment elevation in aVR (≥ 1 mm), minimal ST-segment depression in the inferior leads and from V3 to V6; these discrete alterations could raise the suspicion of LMCA disease and some degree of LSFb. Note: this ECG was considered “normal” by the clinician!! B) Coronary angiography in right anterior oblique cranial projection: this view shows a critical sub-occlusion of the LMCA (arrow) in the middle portion.

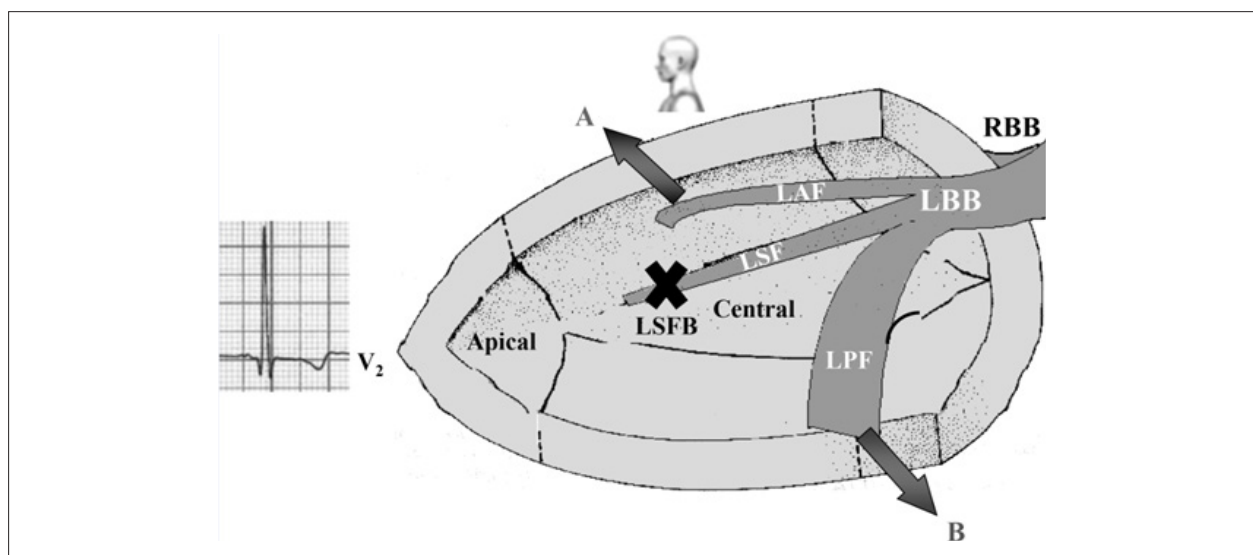


Figure 3 – Outline showing the initial ventricular activation in cases of LSFb. Left His system with its three divisions, in a left sagittal projection. The LAF ends at the base of the ALPM of the mitral valve. The LPF ends in the base of the PMPM of the mitral valve. Since the activation vectors dependent on the anterosuperior (A) and posteroinferior (B) fascicles go in opposite directions, they cancel each other, with minimal predominance of LPF. This phenomenon explains the frequent initial q wave in the right precordial leads in the presence of LPFB. Note the absence of the first 1_{AM} vector, dependent on LSF. LBB: left bundle branch; RBB: right bundle branch; LAF: left anterior fascicle; LPF: left posterior fascicle; LSF: left septal fascicle; LSFB: left septal fascicular block.

Case Report

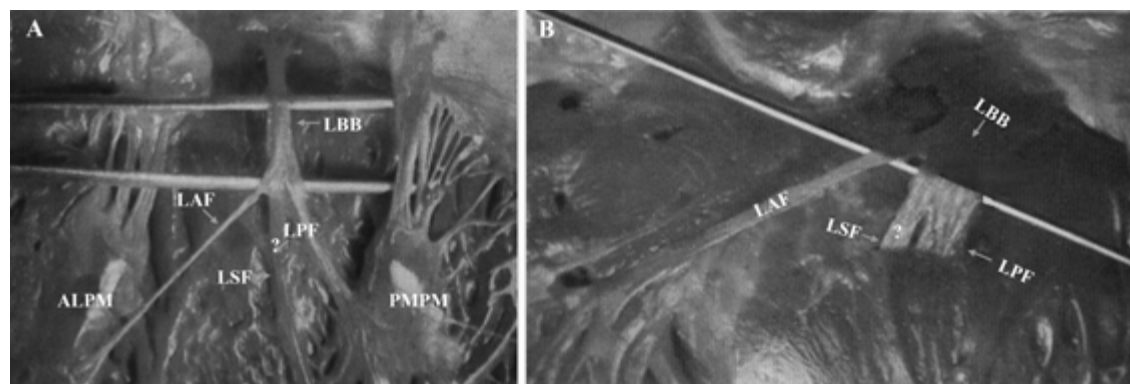


Figure 4 – Endocardial lateral view of the IVS in the human heart.¹¹ In this example the LSF originates from the main LBB. Additionally, the LAF conducts to the ALPM of the mitral valve and the LPF straight to the PMPM of the mitral valve (A). Figure extracted from the original book by Rosenbaum,¹¹ the LSF originates from the LPF. Rosenbaum considered these as “false sinews or tendons” originating from the LPF (B). LBB: left bundle branch; RBB: right bundle branch; LAF: left anterior fascicle; LPF: left posterior fascicle; LSF: left septal fascicle; LSFB: left septal fascicular block.

Left septal fascicle (LSF): it is irrigated exclusively by the septal perforating artery from the LAD, which supplies the upper $\frac{2}{3}$ portion of the interventricular septum (IVS) at this site. Most of the blood supply to the IVS is provided by the LAD. Branches into the septum from the posterior descending artery rarely penetrate more than 10 mm from the epicardium (slightly more than the normal thickness of the LV free wall), so that for practical purposes one may consider the entire blood supply of the IVS to be derived from four to six nearly equal size septal perforating branches of the LAD (Table 1).

In the recent Brazilian consensus paper, the following criteria for LSFB were established. They are as follows, with modifications and clarifying comments by our group:

Presence of prominent anterior forces (PAFs) of the QRS, being transient in sequential tracings. The transitory nature of PAF and the leads involved in it indicate a high likelihood of critical proximal obstruction of the left anterior descending coronary artery (LAD). When this pattern is observed in the scenario of acute coronary syndrome or during a stress test, urgent coronary angiography should be considered;

Normal QRS duration or discrete increase (up to 110 ms) when not associated to other blocks;

Unaltered frontal plane leads;

R-wave-peak time in V1 and V2 ≥ 40 ms.¹⁶ (Note: the term intrinsicoid deflection is not recommended,¹⁷

R-wave voltage in V1 ≥ 5 mm;

R/S ratio in V1 and V2 > 2 ;

S-wave depth in V2 < 5 mm;

Possible heart-rate dependent, embryonic and/or transient q wave¹⁸ in V2 or V1 and V2;

R-wave voltage in V2 > 15 mm;

RS or Rs patterns in V2 and V3 (frequently, rS in V1) with R wave “in crescendo” from V1 through V3 and decreasing from V5 to V6;

Absence of q wave in V5, V6 and I (by absence of 1_{AM} septal vector)¹⁸; confirmed experimentally in explanted human hearts by Durrer et al.¹⁹

Conclusion

To our knowledge, this is the first case in the literature describing ECG features compatible with LSFB associated with LMCA subocclusion. This evolution should alert clinicians about the possibility of severe coronary artery disease in patients with an ECG pattern of LSFB associated with wide-spread ST-segment depression both in patients with stable angina and those with acute coronary syndrome. Coronary angiography without delay should be considered.

Author contributions

Conception and design of the research and Analysis and interpretation of the data: Pérez-Riera AR, Barbosa-Barros R; Writing of the manuscript: Pérez-Riera AR; Critical revision of the manuscript for intellectual content: Pérez-Riera AR, Barbosa-Barros R, Raimundo RD, Abreu LC, Almeida MC, Nikus K.

Potential Conflict of Interest

No potential conflict of interest relevant to this article was reported.

Table 1 – Artery responsible for the irrigation of the three fascicles of the LBB

Responsible system	LAF	LPF	LSF
LAD only	40%	10%	100%
LAD & RCA	50%	40%	0%
RCA only	10%	50%	0%

Sources of Funding

There were no external funding sources for this study.

Study Association

This study is not associated with any thesis or dissertation work.

Ethics approval and consent to participate

This article does not contain any studies with human participants or animals performed by any of the authors.

References

1. Nikus KC, Eskola MJ. Electrocardiogram patterns in acute left main coronary artery occlusion. *J Electrocardiol.* 2008;41(6):626-9.
2. Avula HR, Rassi AN. The Current State of Left Main Percutaneous Coronary Intervention. *Curr Atheroscler Rep.* 2018;20(1):3.
3. Vyas PM, Prajapati JS, Sahoo SS, Patel IV, Deshmukh JK, Patel C, et al. Study of Short and Intermediate Term Clinical Outcomes of Patients with Protected and Unprotected LMCA Stenting. *J Clin Diagn Res.* 2017;11(4):OC29-OC33.
4. Elizari MV, Acunzo RS, Ferreiro M. Hemiblocks revisited. *Circulation.* 2007;115(9):1154-63.
5. Prieto-Solis JA, Benito N, Martin-Duran R. [Electrocardiographic diagnosis of left main coronary artery obstruction using ST-segment and QRS-complex vector analysis]. *Rev Esp Cardiol.* 2008;61(2):137-45.
6. Perez-Riera AR, Barbosa-Barros R, Daminello-Raimundo R, de Abreu LC, Nikus K. Transient left septal fascicular block and left anterior fascicular block as a consequence of proximal subocclusion of the left anterior descending coronary artery. *Ann Noninvasive Electrocardiol.* 2018:e12546.
7. Perez-Riera AR, Barbosa-Barros R, Lima Aragao W, Daminello-Raimundo R, de Abreu LC, Tonussi Mendes Rossette do Valle JE, et al. Transient left septal fascicular block in the setting of acute coronary syndrome associated with giant slurring variant J-wave. *Ann Noninvasive Electrocardiol.* 2018;23(6):e12536.
8. Perez-Riera AR, Nadeau-Routhier C, Barbosa-Barros R, Baranchuk A. Transient Left Septal Fascicular Block: An Electrocardiographic Expression of Proximal Obstruction of Left Anterior Descending Artery? *Ann Noninvasive Electrocardiol.* 2016;21(2):206-9.
9. Riera AR, Ferreira C, Ferreira Filho C, Dubner S, Schapachnik E, Uchida AH, et al. Wellens syndrome associated with prominent anterior QRS forces: an expression of left septal fascicular block? *J Electrocardiol.* 2008;41(6):671-4.
10. Penalzoa D, Tranchesi J. The three main vectors of the ventricular activation process in the normal human heart. I. Its significance. *Am Heart J.* 1955;49(1):51-67.
11. Rosenbaum MB, Elizari MV, Lazzari JO. Los hemibloqueos. Buenos Aires: Editora Paidós; 1967.
12. Frink RJ, James TN. Normal blood supply to the human His bundle and proximal bundle branches. *Circulation.* 1973;47(1):8-18.
13. Bosch X, Theroux P, Roy D, Moise A, Waters DD. Coronary angiographic significance of left anterior fascicular block during acute myocardial infarction. *J Am Coll Cardiol.* 1985;5(1):9-15.
14. James TN. Anatomy of the coronary arteries in health and disease. *Circulation.* 1965;32(6):1020-33.
15. Rokey R, Chahine RA. Isolated left posterior fascicular block associated with acquired ventricular septal defect. *Clin Cardiol.* 1984;7(6):364-9.
16. Perez-Riera AR, de Abreu LC, Barbosa-Barros R, Nikus KC, Baranchuk A. R-Peak Time: An Electrocardiographic Parameter with Multiple Clinical Applications. *Ann Noninvasive Electrocardiol.* 2016;21(1):10-9.
17. Surawicz B, Childers R, Deal BJ, Gettes LS, Bailey JJ, Gorgels A, et al. AHA/ACCF/HRS recommendations for the standardization and interpretation of the electrocardiogram: part III: intraventricular conduction disturbances: a scientific statement from the American Heart Association Electrocardiography and Arrhythmias Committee, Council on Clinical Cardiology; the American College of Cardiology Foundation; and the Heart Rhythm Society. Endorsed by the International Society for Computerized Electrocardiology. *J Am Coll Cardiol.* 2009;53(11):976-81.
18. Gambetta M, Childers RW. Rate-dependent right precordial Q waves: "septal focal block". *Am J Cardiol.* 1973;32(2):196-201.
19. Durrer D, van Dam RT, Freud GE, Janse MJ, Meijler FL, Arzbacher RC. Total excitation of the isolated human heart. *Circulation.* 1970;41(6):899-912.



This is an open-access article distributed under the terms of the Creative Commons Attribution License

Myocardial Involvement in Sweet Syndrome: A Rare Finding in a Rare Condition

Luís Graça-Santos,¹ Katarina Kieselova,² Fernando Montenegro-Sá,¹ Joana Guardado,² João Morais²

Department of Cardiology, Leiria Hospital Centre,¹ Leiria - Portugal

Department of Dermatology, Leiria Hospital Centre,² Leiria - Portugal

Introduction

Sweet Syndrome is an acute febrile neutrophilic dermatosis characterized by an association of fever, neutrophilia, tender erythematous skin lesions (papules, nodules, and plaques), as well as pathologic findings consisting predominantly of mature neutrophils typically located in the upper dermis.¹ It is a rare condition with a worldwide distribution which can present as one of three main clinical types: idiopathic, malignancy-associated, or drug-induced.¹⁻³ Extracutaneous manifestations may occur but cardiovascular involvement is extremely rare.^{1,2}

Case presentation

A previously healthy 41-year-old male presents to the emergency department with a 48-hour history of mild fever and worsening widespread skin lesions. He denied recent drug intake, known allergies, relevant personal or familial diseases, as well as suspicious epidemiological context.

The patient was febrile (38.3°C) and heart rate, blood pressure, and oxygen saturation were all normal. The chest and abdominal examination were both unremarkable. Skin examination revealed painful pseudovesiculate, erythematous papules, and plaques on the nape, neck, shoulders, and arms, as well as painful hyperpigmented subcutaneous nodules (erythema nodosum-like) on the legs (Figure 1). Blood tests showed slight leucocytosis (10800/uL) with 81.4% of neutrophils, erythrocyte sedimentation rate was 89mm/h (normal value (NV) <10) and C-reactive protein (CRP) 128.5mg/L (NV<5.0). Electrolytes, renal and hepatic profiles were normal.

A few hours later, the patient complained of transient chest discomfort at rest. The electrocardiogram showed sinus rhythm at 58 per minute with first-degree atrioventricular block plus incomplete right bundle branch block. Troponin I (TnI) was 1.89ng/mL (NV<0.05) and raised up to 10.82ng/mL six hours later. The repeated electrocardiogram was identical to the previous one. Transthoracic echocardiogram (TTE) was



Figure 1 – Skin examination. Pseudovesiculate, erythematous papules and plaques on the nape (top); hyperpigmented subcutaneous nodules on the legs (bottom).

normal, demonstrating preserved left ventricular ejection fraction (LVEF; 53% Simpson's biplane method) with no major wall motion abnormalities. However, global longitudinal peak systolic strain (GLPSS) was reduced, especially at the expense of the mid-basal segments being the apex relatively spared (Figure 2.A). Coronary angiogram excluded obstructive coronary artery disease (CAD).

The patient was admitted to the internal medicine ward with the presumptive diagnosis of acute febrile neutrophilic dermatosis. On the second day (D2), skin biopsy was performed and oral prednisolone (PDN) 1mg/Kg/day was initiated, taking into consideration the persistence of both fever and skin lesions as well as the increase of the CRP value (242mg/L). Despite no chest discomfort relapse, TnI reached a peak level of 15.01ng/mL on D2. After initiating PDN, the patient remained afebrile, and both systemic inflammatory and myocardial injury biomarkers started to decrease. Complementary laboratorial tests (such as electrophoretic proteinogram, autoimmunity screening, thyroid hormones, blood cultures and serology tests) were normal. The histological skin analysis revealed subepithelial oedema, dermal inflammatory infiltrate with polymorphonuclear predominance and absence of vasculitis (Figure 3). Based on this information, diagnostic criteria

Keywords

Sweet Syndrome/physiopathology; Erythema Multiforme; Neutrophils; Myocarditis; Adrenal Cortex Hormones/therapeutic use.

Mailing Address: Luís Graça Santos •

Leiria Hospital Centre - Rua Santo Andre Pousos. 2410-196, Leiria – Portugal

E-mail: luismscp1@gmail.com

Manuscript received April 13, 2019, revised manuscript July 27, 2019, accepted August 18, 2019.

DOI: <https://doi.org/10.36660/abc.20190249>

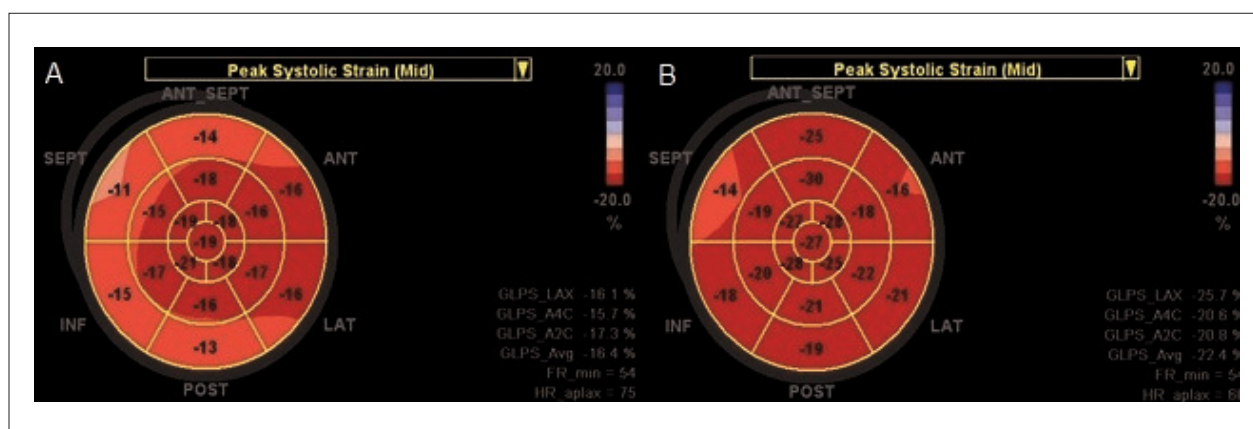


Figure 2 – Global and segmental longitudinal strain analysis; “bull-eye” plot (General Electric®). (A) Global strain is reduced (-16.4%) at admission; (B) and normalized (-22.4%) three months after corticosteroid treatment.

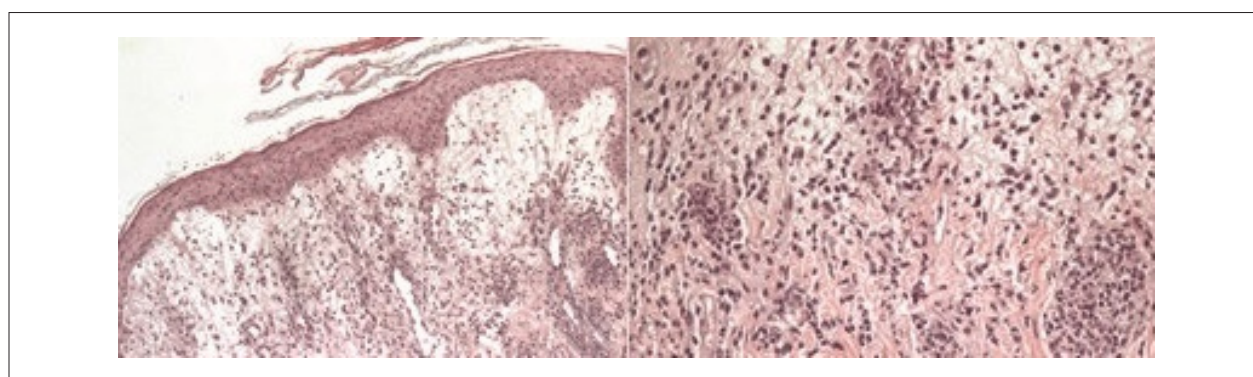


Figure 3 – Histology of the cervical skin lesion (haematoxylin-eosin stain). Predominant neutrophilic dermal infiltrate and oedema (left). Zoom over the dermal area showing some lymphocytes, histiocytes, and absence of vasculitis (right).

were fulfilled for SS³ and a high likelihood for cardiovascular involvement presenting as acute myocarditis (AM)³ was considered. On D9, there had been no fever relapse, skin lesions were mostly healed, and CRP and TnI levels almost normalized (9.9mg/L and 0.32ng/dL respectively). The patient was discharged on a tapering corticosteroid regimen.

Four days later, the patient presented completely asymptomatic with no skin lesions and both systemic inflammatory and myocardial injury biomarkers have normalized. A cardiovascular magnetic resonance (CMR) was scheduled six days after discharge and showed findings suggestive of myocarditis (Figure 4). Both LVEF and GLPSS improved up to 63% and -22.4%, respectively, three months after the initial assessment (Figure 2.B). The patient did not wish to undergo a second CMR study.

During a two-year follow-up, the patient remained completely asymptomatic with no signs or symptoms of cardiovascular or malignant disease.

Discussion

We present a case where the diagnosis of SS was established as two major and three minor Driesch criteria were identified.⁴

The idiopathic type was assumed since no recent drug intake was reported and no signs of malignant disease were present. Extracutaneous manifestations may occur, particularly in association with malignancy.^{1,2} Cardiovascular involvement is extremely rare and up to this date, only two cases of myocarditis have been reported in the idiopathic type, to our best knowledge.^{2,5,6} Both manifestations typically respond well to corticosteroids.¹

In this patient, the presence of transient chest discomfort associated with TnI elevation raised the suspicion of cardiovascular involvement. Both AM and acute myocardial infarction have been previously described as cardiovascular manifestations.² Coronary angiogram remains the gold standard for the diagnosis of CAD⁷ or for its exclusion in case of suspected AM⁸ and was normal in this case. There is some evidence that two-dimensional speckle tracking echocardiography (2D-STE) may help support the diagnosis of AM since GLPSS correlates with the presence of fibrosis and oedema on CMR and with lymphocytic infiltrates on endomyocardial biopsy (EMB).⁹⁻¹² In our case, the presence of GLPSS reduction mainly at the expense of the mid-basal segments, instead of the mid-apical segments (typical

Case Report

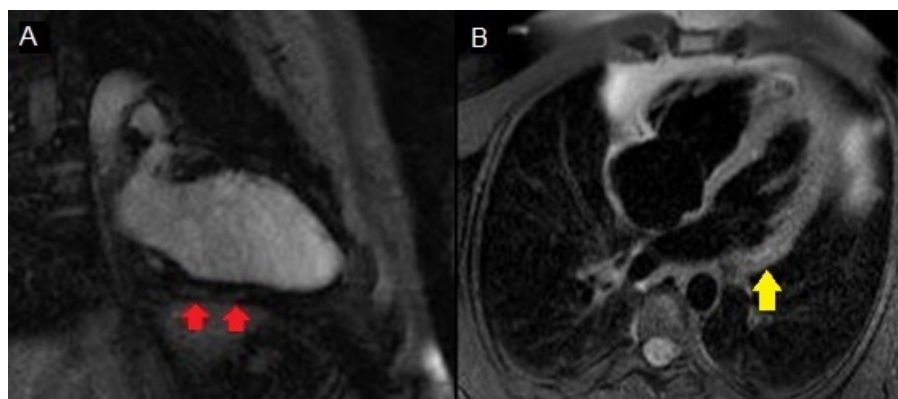


Figure 4 – Cardiovascular magnetic resonance imaging. (A) T1-weighted image demonstrating patchy subepicardial late gadolinium enhancement (red arrows) in the basal portion of the inferior wall; (B) T2-weighted image presenting focal regions of increased signal intensity (yellow arrow) suggestive of slight oedema in the inferolateral wall.

pattern of significant CAD),¹³ and the prompt response to corticosteroids raised the likelihood of AM. Due to clinical stability and the well-known limitations of EMB, a CMR was later performed and suggested this diagnosis according to the Lake-Louise criteria.^{8,12} In fact, CMR has emerged as a useful non-invasive diagnostic tool and there is growing evidence that novel techniques, such as T1 and T2 mapping, may improve its diagnostic accuracy for myocarditis and help monitor disease evolution.^{8,14,15} Additionally, GLPSS normalized three months after treatment, while the patient remained asymptomatic.

Final messages

The case we present emphasizes the importance of acknowledging SS as a rare yet plausible cause of cardiovascular disease, and one that should be early recognized in order to start adequate treatment.

In this case, the diagnosis of AM was highly suggested by the combination of non-invasive imaging modalities after CAD exclusion. To our best knowledge, this was the first time CMR was used to assess myocardial involvement in a patient with SS and also the first to report the use of 2D-STE for evolution

monitoring. Both cutaneous and cardiovascular manifestations completely regressed after corticosteroid treatment.

Author contributions

Conception and design of the research and Data acquisition: Santos LG, Kieselova K; Analysis and interpretation of the data: Santos LG, Kieselova K, Sá FM, Guardado J; Writing of the manuscript: Santos LG, Sá FM, Morais JA; Critical revision of the manuscript for intellectual content: Guardado J, Morais JA.

Potential Conflict of Interest

The authors report no conflict of interest concerning the materials and methods used in this study or the findings specified in this paper.

Sources of Funding

There was no external funding source for this study.

Study Association

This study is not associated with any thesis or dissertation.

References

1. Cohen PR. Sweet's syndrome - a comprehensive review of an acute febrile neutrophilic dermatosis. *Orphanet J Rare Dis*. 2007 jul 26;2:34.
2. Villarreal-Villarreal CD, Ocampo-Candiani J, Villarreal-Martínez A. Sweet Syndrome: A Review and Update. *Actas Dermosifiliogr*. 2015;107(5):369-78.
3. Cohen PR, Kurzrock R. Sweet's syndrome revisited: a review of disease concepts. *Int J Dermatol*. 2003;42(10):761-78.
4. Von den Driesch P. Sweet's syndrome (acute febrile neutrophilic dermatosis). *J Am Acad Dermatol*. 1994;31(4):535-56.
5. Dorenkamp M, Weikert U, Meyer R, Schwimbeck PL, Morguet AJ. Heart failure in acute febrile neutrophilic dermatosis. *Lancet*. 2003;362(9393):1374.
6. Yu WY, Manriquez E, Bhutani T, Chaganti RK, Ruben BS, Schwartz BS, et al. Sweet heart: A case of pregnancy-associated acute febrile neutrophilic dermatosis with myopericarditis. *JAAD Case Rep*. 2014;1(1):12-4.
7. Montalescot G, Sechtem U, Achenbach S, Sechtem U, Andreotti F, Arden C, et al. 2013 ESC guidelines on the management of stable coronary artery disease: the Task Force on the management of stable coronary artery disease of the European Society of Cardiology. *Eur Heart J*. 2013;34(38):2949-3003.
8. Caforio AL, Pankuweit S, Arbustini E, Basso C, Gimeno-Blanes J, Felix SB, et al. Current state of knowledge on aetiology, diagnosis, management, and therapy of myocarditis: a position statement of the European Society of Cardiology Working Group on Myocardial and Pericardial Diseases. *Eur Heart J*. 2013;34(33):2636-48.

9. Leitman M, Vered Z, Tyomkin V, Macogon B, Peleg E, Copel L. Speckle tracking imaging in inflammatory heart diseases. *Int J Cardiovasc Imaging*. 2018;34(5):787-92.
10. Kostakou PM, Kostopoulos VS, Tryfou ES, Giannaris VD, Rodis IE, Olympios CD, et al. Subclinical left ventricular dysfunction and correlation with regional strain analysis in myocarditis with normal ejection fraction. A new diagnostic criterion. *Int J Cardiol*. 2018;259:116-21.
11. Løgstrup BB, Nielsen JM, Kim WY, Poulsen SH. Myocardial oedema in acute myocarditis detected by echocardiographic 2D myocardial deformation analysis. *Eur Heart J Cardiovasc Imaging*. 2016;17(9):1018-26.
12. Escher F, Kasner M, Kühl U, Heymer J, Wilkenshoff U, Tschöpe C, et al. New echocardiographic findings correlate with intramyocardial inflammation in endomyocardial biopsies of patients with acute myocarditis and inflammatory cardiomyopathy. *Mediators Inflamm*. 2013;2013:875420.
13. Carstensen HG, Larsen LH, Hassager C, Kofoed KF, Jensen JS, Mogelvang R. Association of ischemic heart disease to global and regional longitudinal strain in asymptomatic aortic stenosis. *Int J Cardiovasc Imaging*. 2015;31(3):485-95.
14. André F, Stock FT, Riffel J, Giannitsis E, Steen H, Scharhag J, et al. Incremental value of cardiac deformation analysis in acute myocarditis: a cardiovascular magnetic resonance imaging study. *Int J Cardiovasc Imaging*. 2016;32(7):1093-101.
15. Roller FC, Harth S, Schneider C, Krombach GA. T1, T2 Mapping and Extracellular Volume Fraction (ECV): Application, Value and Further Perspectives in Myocardial Inflammation and Cardiomyopathies. *Rofo*. 2015 Sep;187(9):760-70.



This is an open-access article distributed under the terms of the Creative Commons Attribution License

Idiopathic Left-Bundle Branch Block and Unexplained Symptom At Exercise: A Case Report

Guilherme Veiga Guimarães¹ e Edimar Alcides Bocchi¹

Universidade de São Paulo Instituto do Coração, 1 São Paulo, SP – Brasil

Introduction

The presence of a left bundle branch block (LBBB) in the apparent absence of any other heart disease raises questions and concerns about the stratification of the risk of subsequent cardiovascular events or symptoms.¹⁻⁵ The detection of LBBB in asymptomatic adults, including athletes, is estimated to range between 0.1% and 0.8%, which is more likely to represent a structural heart disease rather than a physiological response to exercise.⁶⁻⁸ On the other hand, some studies have shown that the mortality risk of patients with LBBB and heart disease varies between 2.4% and 11% per year.⁹

Although several studies have suggested that exercise-induced LBBB is usually associated with cardiovascular disease and, particularly, coronary artery disease, there are contrasting studies showing an association between exercise-induced LBBB and normal coronary arteries.^{6,7,9} However, exercise-related cardiovascular adverse effects in LBBB with normal resting cardiac function remains poorly defined.

This case report examined the relationship between exercise, LBBB, symptoms and exercise capacity in a younger woman, with typical LBBB and without history of cardiovascular disease, who reported sudden anxiety and shortness of breath during vigorous exercise, which can be suggestive of cardiac disease, being referred for exercise stress testing.

Case Report

A healthy 42-year-old woman with LBBB, who reported sudden anxiety and shortness of breath during vigorous exercise, and was referred for cardiopulmonary exercise testing (CPX) to evaluate the unexplained symptoms. She was not taking any medication and had no significant medical history. She had no previous symptoms suggestive of cardiac disease (chest discomfort, palpitations, fainting and angina). She had no history of neuromuscular or pulmonary disease. She did not smoke or drink alcohol. There was no family

history of cardiac disease or heart attack. Over the previous 6 months, she had been exercising three times a week at the gym. The exercise program consisted of sessions of at least 60 min of regular activity at moderate intensity, including aerobic, muscle-strengthening, flexibility, and balance-strengthening exercises. Her physical examination was considered normal, her BMI was 21.5 kg/m² and her resting blood pressure was 110/70 mmHg. The resting electrocardiogram (ECG) showed a sinus rhythm (SR) and heart rate (HR) of 70 bpm, with the dominant feature of intraventricular block: prolonged QRS complex (≥ 0.12 s) due to delayed activation of the left ventricle, accompanied by a characteristic morphology of the QRS complex.⁶ Coronary computed tomography angiography (CTA) was performed, which showed no deposits of calcium and fatty material in the coronary arteries and no stenotic coronary arteries. A complete blood count showed normal results: her fasting glucose was 78 mg/dL, low-density lipoprotein cholesterol (LDL-C) was 168 mg/dL, high-density lipoprotein cholesterol (HDL-C) was 81 mg/dL, total cholesterol was 159 mg/dL, lipoprotein(a) [Lp(a)] was 7 mg/dL, triglycerides were 49 mg/dL and creatine phosphokinase (CPK) was 26 U/L. The magnetic resonance imaging (MRI) of the heart showed normal biventricular function, a left ventricular ejection fraction of 65% and preserved dimensions, except for an abnormal septal motion.

She underwent CPX on a treadmill. Throughout the CPX phases, the 12-lead ECG showed a SR (Figure 1). Blood pressure measurements were in the normal range: at rest (126/82 mmHg), peak exercise (160/90 mmHg) and recovery stages (120/90 mmHg). She stopped the exercise due to fatigue (RER=1.29). Peak oxygen consumption ($\text{VO}_{2\text{peak}}$ = 27.1 ml/kg/min) and maximum heart rate (HR_{max} = 176 bpm) values obtained from CPX were normal for age and gender, 95% and 102%, respectively. (<https://www.ahajournals.org/doi/10.1161/01.CIR.91.2.580>) From stage 14 of the modified Balke protocol until test termination, the CPX identified a decrease in VO_2 and in O_2 pulse (VO_2/HR , ml/bpm), and an increase in HR and dead space to tidal volume ratio (Vd/Vt) (Figure 2). From this event, the minute ventilation/carbon dioxide production relationship slope (VE/VCO_2 slope) increased abruptly and was not accompanied by hypoxia (Figure 2).

Keywords

Bundle Branch Block; Exercise; Physical Activity; Oxygen Consumption/physiology; Cardiovascular Diseases/prevention and control.

Mailing Address: Guilherme Veiga Guimarães •

Universidade de São Paulo Instituto do Coração – Av. Dr. Eneas de Carvalho Aguiar, 44. Postal Code 05403-000, São Paulo, SP – Brazil

E-mail: gvguima@usp.br

Manuscript received June 05, 2019, revised manuscript July 25, 2019, accepted September 10, 2019

DOI: <https://doi.org/10.36660/abc.20190363>

Discussion

To the best of our knowledge, we report for the first time a younger woman with LBBB without apparent cardiomyopathy and with unexplained symptoms during vigorous exercise (decreased VO_2 , during CPX), which is suggestive of impaired cardiac function in the face of cardiovascular stress. There were no ECG abnormalities except for a LBBB. Heart rate reserve and blood pressure were normal throughout the CPX test.

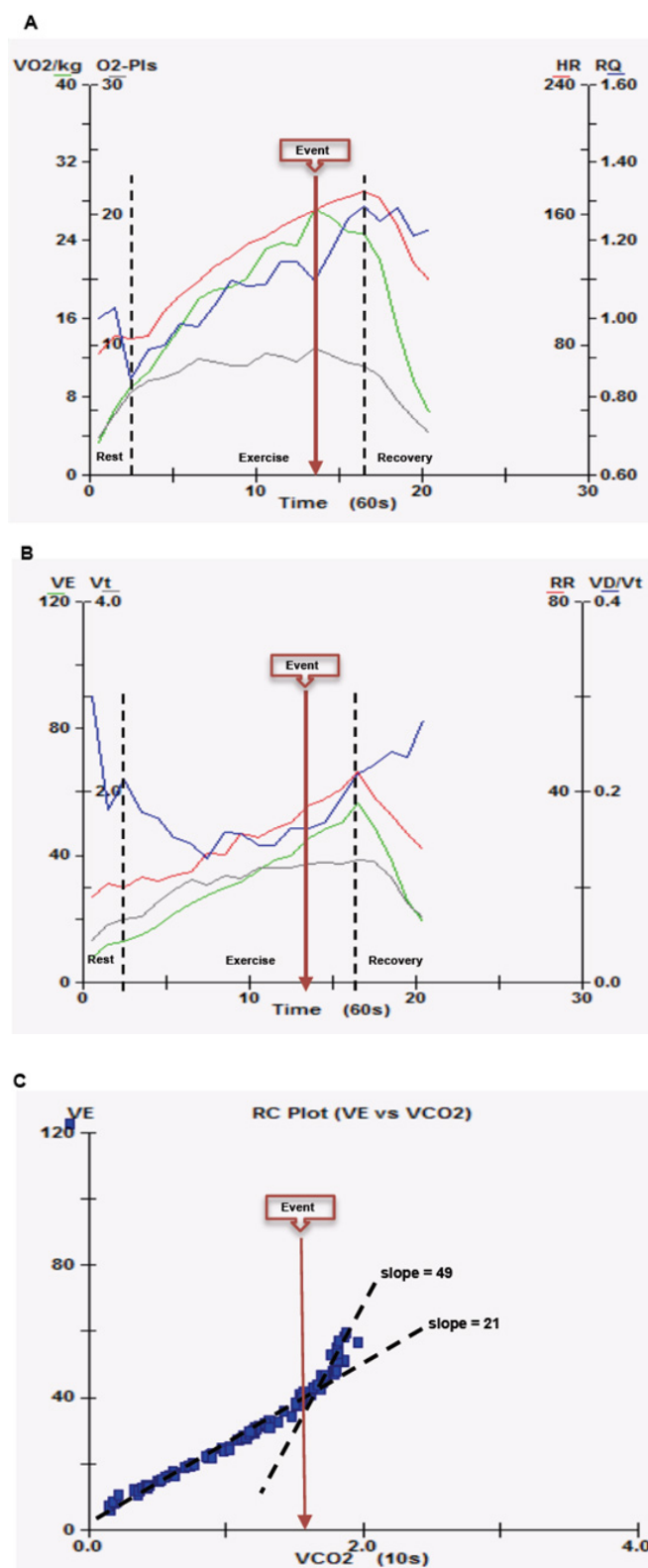


Figure 1 – Cardiopulmonary exercise test at rest, during exercise and recovery. The black lines indicate the transition between these phases. A) green line - oxygen consumption (VO₂/kg, ml/kg/min), red line - heart rate (HR, bpm), black line - oxygen pulse (O₂-Pls, ml/bpm) and blue line - respiratory coefficient (RQ); B) green line - minute ventilation (VE, l/min), red line - respiratory rate (RR, bpm), black line - tidal volume (Vt, ml/min) and blue line - dead space to tidal volume ratio (Vd/Vt). C) Minute ventilation/carbon dioxide production relationship slope (VE/VCO₂ slope). In the first part of the exercise, VE/VCO₂ slope is normal (21); from the event point during the exercise test, the VE/VCO₂ slope severely increased (49). Brown line arrow - event point.

Case Report

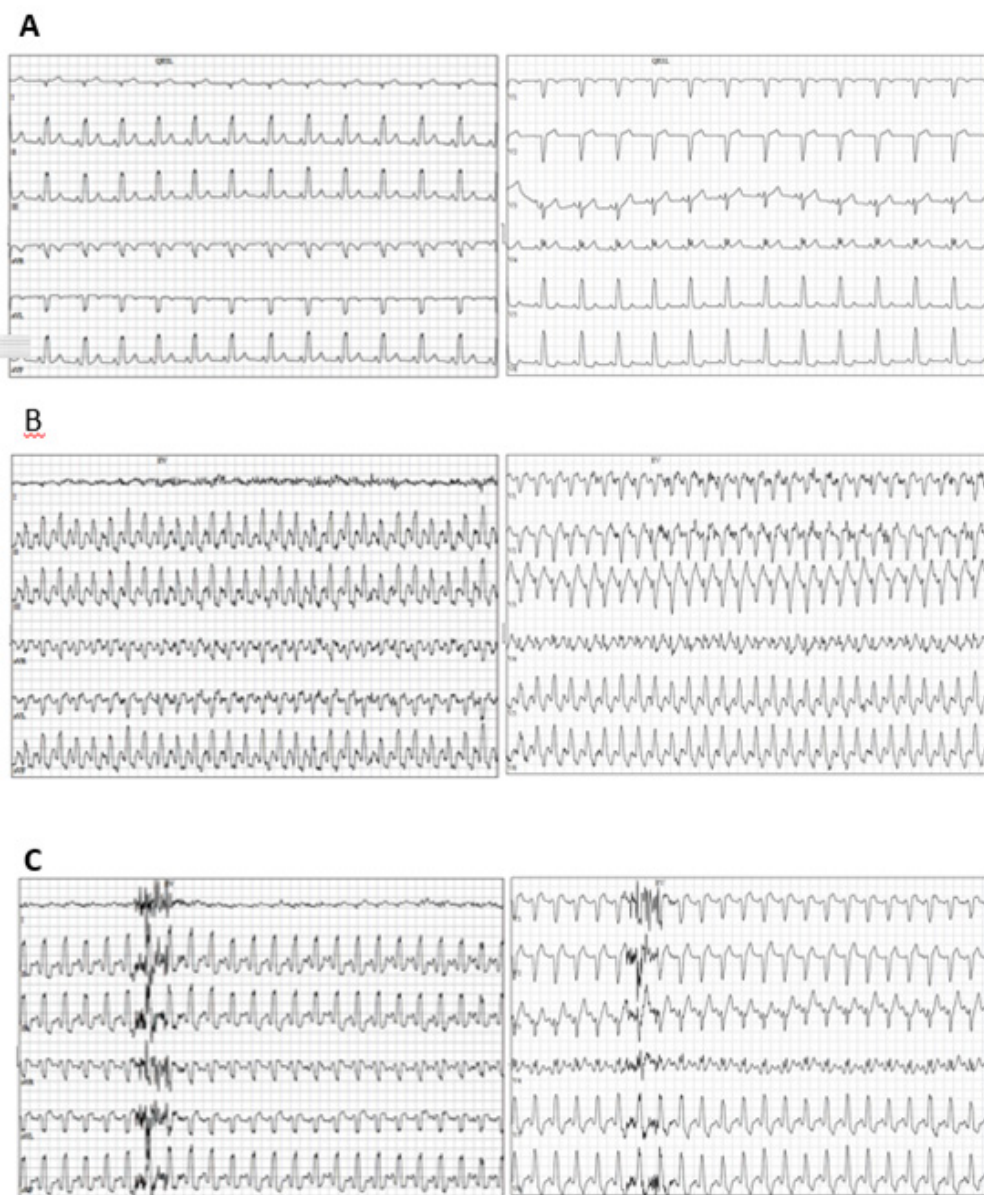


Figure 2 – Electrocardiogram demonstrating left bundle branch block: a resting rate of 75 bpm (A), a heart rate of 175 bpm during maximal exercise tolerance test (B) and a heart rate 153 bpm in the first minute of the recovery period (C).

Exercise provides a useful tool for the indirect assessment of cardiac functional reserve, from left ventricular performance, the change from rest to peak exercise, and can be limited in the presence of disease. In this context, a drop in the cardiovascular pattern of VO_2 responses may represent impaired cardiac output (CO) or impaired peripheral oxygen extraction as is observed in heart failure.¹⁰ On the other hand, in healthy individuals, the level to which oxygen consumption and peripheral oxygen extraction increase in response to exercise is much greater compared to changes in stroke volume and similar to the increase observed in HR.

The decrease in VO_2 and O_2 pulse, in spite of the increase in HR, observed in this case, may indicate a possible cardiac abnormality. We suggest that the asynchronous motion of the left ventricle associated with delayed wall contraction can reduce the left ventricular workload, resulting in a lower stroke volume and indicating a decrease in cardiac output during maximal exercise, despite the increase in HR.⁸⁻¹⁰ This reduction in left ventricular work by an apparent septal perfusion defect during CPX can lead to energy loss and waste of myocardial work, which may represent the hemodynamic impact of asynchronous electrical activation of the myocardium during LBBB,⁸⁻¹⁰ and partly explain the drop of VO_2 observed during

CPX. On the other hand, exercise-induced left bundle branch block may be related or not to apparent cardiac abnormalities. However, patients with this finding have significantly higher all-cause mortality rates compared to those without exercise-induced left bundle branch block.¹¹

This apparent decrease in cardiac function during exercise may be due to a transitory decrease in stroke volume, probably related to worsening left ventricular (LV) function associated with an abrupt increase in the VE/VCO₂ slope, giving rise to a higher dead space to tidal volume ratio and an early increase in the respiratory rate, as compensatory mechanisms.^{1,3,5,10} This disturbance in pathophysiology is linked with LV dysfunction, caused or worsened by LBBB, may indirectly lead to right ventricular dysfunction through increased left-sided filling pressure, causing changes in the function of the lungs' airways, and to the development of abnormal gas exchange due to alveolar-capillary dysfunction.^{3,4} In addition, a higher VE/VCO₂ slope is suggestive of secondary pulmonary hypertension, as a consequence of another primary condition, such as heart failure or pulmonary disease.^{3,4}

Consideration

Cardiopulmonary exercise testing in LBBB, in the absence of other heart diseases, should be considered as a technique to evaluate the exercise capacity in patients with unexplained symptoms.

References

1. Belli JFC, Bacal F, Bocchi EA, Guimarães GV. "Ergoreflex activity in heart failure." *Arq Bras Cardiol*. 2011;97(2):171-8.
2. Breithardt G, Breithardt OL. Left bundle branch block, an old-new entity. *J Cardiovasc Transl Res*. 2012;5(2):107-16.
3. Farina S, Correale M, Bruno N, Paolillo S, Salvioni E, Badagliacca R, et al., Stefania, et al. The role of cardiopulmonary exercise tests in pulmonary arterial hypertension. *Eur Respir Rev*. 2018;27(148):17034.
4. Guazzi M, Cahalin L, Arena R. Cardiopulmonary exercise testing as a diagnostic tool for the detection of left-sided pulmonary hypertension in heart failure. *J Card Fail*. 2013;19(7):461-7.
5. Guimarães GV, Belli JC, Bacal F, Bocchi EA. Behavior of Central and Peripheral Chemoreflexes in Heart Failure. 2011; 96(2):161-7.
6. Kim JH, Baggish AL. Electrocardiographic right and left bundle branch block patterns in athletes: prevalence, pathology, and clinical significance. *J Electrocardiogr*. 2015;48(3):380-4.
7. Kim JH, Baggish AL. Significance of electrocardiographic right bundle branch block in trained athletes. *Am J Cardiol*. 2011;107(7):1083-9.
8. Koepfli P, Wyss C, Gaemperli O, Siegrist PT, Klainuti M, Schepis T, et al. "Left bundle branch block causes relative but not absolute septal underperfusion during exercise. *Eur Heart J*. 2009;30(24): 2993-9.
9. Lamberti M, Ratti G, Di Miscio G, Franciolini E. Cardiovascular risk in young workers with left bundle branch block. *Open J Prev Med*. 2014;4(5):270-4.
10. Lim HS, Hoong S, Theodosiou M. Exercise ventilatory parameters for the diagnosis of reactive pulmonary hypertension in patients with heart failure. *J Card Fail*. 2014;20(9):650-7.
11. Stein R, Ho M, Oliveira CM, Ribeiro JP, Lata K, Abella J, et al. Exercise-induced left bundle branch block: prevalence and prognosis. *Arq Bras Cardiol*. 2011;97(1):26-32.

Author Contributions

Conception and design of the research, Acquisition of data and Critical revision of the manuscript for intellectual content: Guimarães GV; Analysis and interpretation of the data and Writing of the manuscript: Guimarães GV, Bocchi EA.

Potential Conflict of Interest

No potential conflict of interest relevant to this article was reported.

Sources of Funding

GV Guimarães was supported by National Council for Scientific and Technological Development (CNPq:301957/2017-7).

Study Association

This study is not associated with any thesis or dissertation work.

Ethics Approval and Consent to Participate

This article does not contain any studies with human participants or animals performed by any of the authors.



This is an open-access article distributed under the terms of the Creative Commons Attribution License

An Unusual Pacemaker-Induced Tachycardia

Madalena Coutinho-Cruz,¹ Guilherme Portugal,¹ Pedro Silva-Cunha,¹ Mário Martins-Oliveira¹

Centro Hospitalar de Lisboa Central EPE – Cardiologia,¹ Lisboa - Portugal

Case Report

A 29 year-old female patient with double inlet left ventricle, ventricle septal defect, malposition of the great arteries and subpulmonary obstacle, submitted to a modified Fontan procedure, at 9 years of age, presented with severely symptomatic brady-tachy syndrome (palpitations and syncope). Since venous access to the right ventricle was absent (due to the surgical redirection of venous blood flow from the right atrium to the pulmonary artery bypassing the ventricles) and the AV conduction was normal, it was decided to implant a permanent atrial pacemaker. A single active fixation lead was placed in the right atrial lateral wall, due to suboptimal pacing threshold in the atrial appendage. Due to concerns that either the progression of the conduction system disease or the effect of heart rate-slowing medication could lead to AV conduction disease, which would require an epicardial lead later on, a Sorin Reply 200 DR pulse generator with a plug in the ventricular port was used. The day after the procedure, the patient complained of palpitations. Figure 1 shows the ECG tracing performed.

The ECG reveals a repetitive cycle of an atrial paced beat (Ap) and an atrial intrinsic beat (Ai) each followed by a ventricular intrinsic beat (Vi). The Ap-Ap interval is 1000 ms, which is in agreement with the programmed lower rate limit (60 beats per minute). The Ai-Ai interval is also 1000 ms and the Ap-Ai interval is 480 ms, which amounts to a mean effective ventricular rate of 120 bpm. The intrinsic AV interval is 180 ms. There was clearly an undersensing of every other atrial beat. After interrogation of the device, although pacing and sensing threshold were adequate, it was noted that the pacemaker was still in factory settings, in DDD mode instead of the patient's appropriate AAI mode. Figure 2 shows a reproduction of the intracardiac electrograms overlaying the presenting surface ECG.

In the atrial channel, an Ap is followed by an atrial intrinsic beat in the refractory period (Ar), followed again by an Ap. As mentioned before, the ventricular port on the generator was plugged and it was not possible neither to sense nor to pace the ventricle. As such, the ventricular paced beats (Vp) are inconsequential with respect to actual ventricular activation.

Keywords

Pacemaker, Artificial/adverse effects; Sick Sinus Syndrome/ complications; Tachycardia/surgery.

Mailing Address: Madalena Cruz •

Centro Hospitalar de Lisboa Central EPE - Rua de Santa Marta, 50 Lisboa 1150-064 - Portugal

E-mail: madalena.cruz89@gmail.com

Manuscript received February 23, 2019, revised manuscript June 04, 2019, accepted October 23, 2019

DOI: <https://doi.org/10.36660/abc.20190133>

Programmed parameters were: lower rate limit (LRL) 60 bpm; upper tracking rate 120 bpm; post-ventricular atrial refractory period (PVARP) 280 ms; paced AV delay 220 ms.

In a DDD pacemaker, after an Ap, a paced AV delay is started, after which there is either a sensed Vi or a Vp. In these cases, even though there is a Vi through intrinsic nodal conduction, there is no ventricular lead to sense this event. The AV delay is then followed by a Vp that, for the same reason, has no representation in the surface ECG. After the Vp, the post-ventricular atrial refractory period (PVARP) starts. Its main role is to prevent the sensing of retrograde P waves that might trigger a pacemaker mediated tachycardia. The initial component of the PVARP is occupied by the post-ventricular atrial blanking (PVAB), which is absolutely refractory. Beyond the PVAB, the period is relatively refractory. During the PVARP, atrial events are sensed and identified as refractory (Ar) on the event marker channel, though it does not modify the synchronization of the pacing intervals.¹ Thus, the next Ai does not trigger an AV delay and a Vp, as it falls in the PVARP, but is recorded in the intracardiac electrogram as Ar. This Ai is followed by a Vi through intrinsic nodal conduction, which, again, is not sensed. The next Ap is triggered after the ventriculo-atrial (VA) interval starting at the last Vp to maintain the lower rate limit at 60 bpm (in this case, 780 ms). After correctly programming it to AAI mode, the ECG shown in Figure 4 was obtained. It reveals Ap beats at 60 bpm, each followed by a Vi with no intervening Ai.

This unusual kind of “pacemaker-induced tachycardia” is only possible because of the simultaneous occurrence of a set of conditions. Firstly, a pacemaker with a single atrial lead was programmed in a DDD mode. This mode initiated an AV delay after Ap and a PVARP after the Vp. The next Ai is then sensed during the refractory period and does not reset the pacing intervals. Secondly, the absence of a ventricular lead also precludes the Vi after the Ar to be sensed and reset the VA interval. Thirdly, the patient's intrinsic rhythm during this period is timed to occur before the end of the programmed PVARP, so that this interval prevents it from being sensed outside the refractory period. Lastly, the patient's intact AV conduction allows for all Ap and Ar to be conducted to the ventricle and the rate to rise to 120 bpm. Another reported case depicts a similar problem, in which a single atrial lead programmed in DDD mode fails to recognize an episode of atrial tachycardia.² Careful programming and deep understanding of pacing functions are crucial for the management of these patients.

Author contributions

Conception and design of the research and Analysis and interpretation of the data: Portugal G; Acquisition of data and Writing of the manuscript: Coutinho-Cruz M; Critical revision of the manuscript for intellectual content: Silva-Cunha P, Martins-Oliveira M.

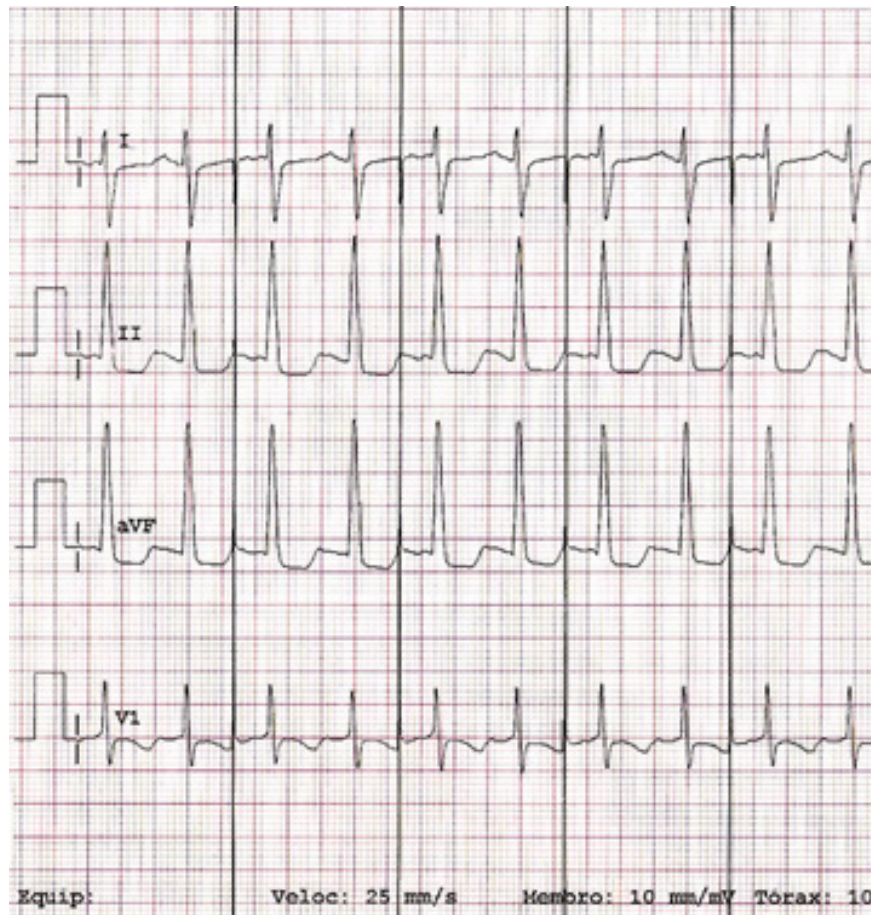


Figure 1 – ECG after pacemaker implantation. Repetitive cycle of an atrial paced beat and an atrial intrinsic beat both followed by a ventricular intrinsic beat.

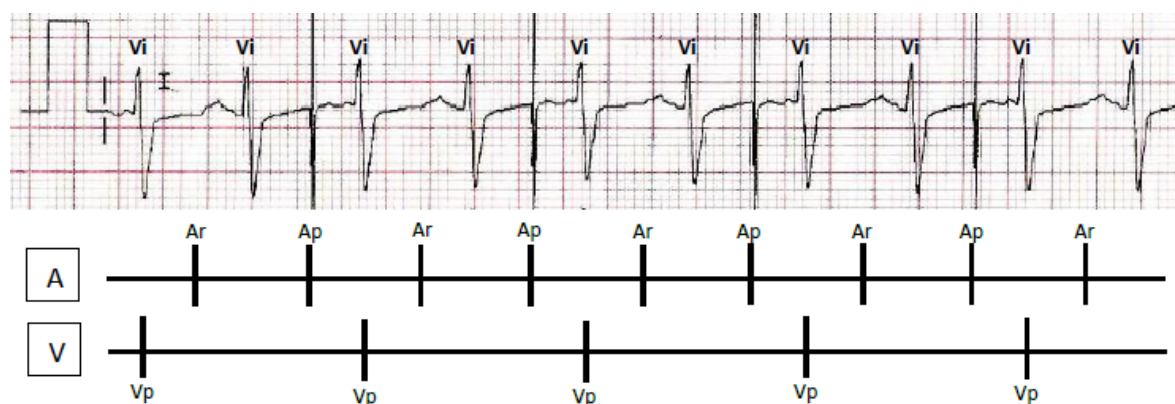


Figure 2 – Reproduction of the intracardiac atrial and ventricular electrograms overlaying lead I of the presenting surface ECG. A: atrial channel. Ap: atrial paced event. Ar: atrial event sensed in the refractory period. V: ventricular channel. Vi: intrinsic ventricular event. Vp: ventricular paced event.

Case Report

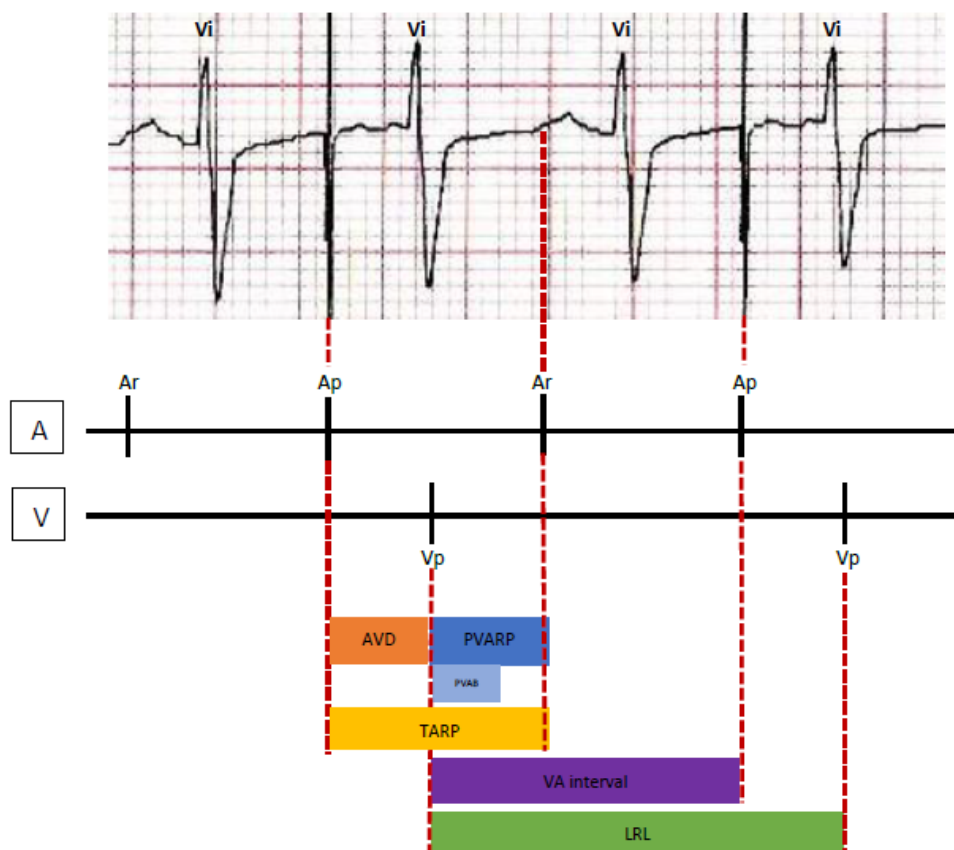


Figure 3 – Representation of the pacing intervals of the pacemaker in DDD mode. A, atrial channel. Ap, atrial paced event. Ar, atrial event sensed in the refractory period. AVD, AV delay. LRL, lower rate limit. PVAB, post-ventricular atrial blanking. PVARP, post-ventricular atrial refractory period. TARP, total atrial refractory period. V, ventricular channel. VA interval, ventriculo-atrial interval. Vi, intrinsic ventricular event. Vp, ventricular paced event.

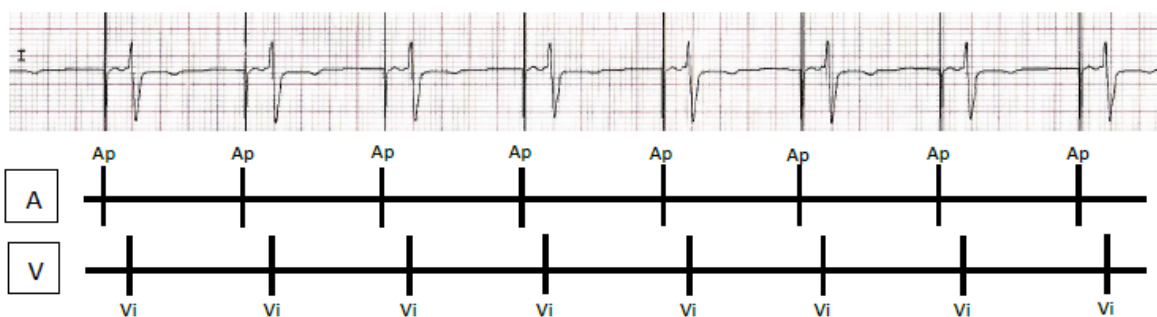


Figure 4 – Reproduction of the intracardiac atrial and ventricular electrograms overlaying lead I of the surface ECG after reprogramming of the pacemaker. A, atrial channel. Ap, atrial paced event. V, ventricular channel. Vi, intrinsic ventricular event.

Potential Conflict of Interest

No potential conflict of interest relevant to this article was reported.

Sources of Funding

There were no external funding sources for this study.

Study Association

This study is not associated with any thesis or dissertation work.

Ethics approval and consent to participate

This article does not contain any studies with human participants or animals performed by any of the authors.

References

1. Kenny T. The Nuts and Bolts of Implantable Device Therapy Pacemakers. Hoboken(NJ): Wiley-Blackwell; 2015.
1. Noheria, A, Friedman, PA, Asirvatham, SJ, McLeod, CJ. Dual chamber pacing mode in an atrial antitachycardia pacing device without a ventricular lead - A necessary evil. Indian Pacing and Electrophysiology J 2015;15(2):133-7.



This is an open-access article distributed under the terms of the Creative Commons Attribution License

Spontaneous Coronary Artery Dissection in a Patient with Cerebrotendinous Xanthomatosis

Maria Júlia Silveira Souto,¹ Marcos Antônio Almeida-Santos,^{2,3} Eduardo José Pereira Ferreira,^{1,3} Luiz Flávio Galvão Gonçalves,^{1,3} Joselina Luzia Menezes Oliveira,^{1,3} Antônio Carlos Sobral Sousa^{1,3}

Universidade Federal de Sergipe,¹ São Cristóvão, SE - Brazil

Programa de Pós-Graduação em Saúde e Meio Ambiente, Universidade Tiradentes,² Aracaju, SE - Brazil

Centro de Educação e Pesquisa da Fundação São Lucas,³ Aracaju, SE - Brazil

Introduction

Cerebrotendinous xanthomatosis (CTX) is an autosomal recessive disease characterized by the formation of xanthomatous lesions in many tissues, particularly the brain and tendons.¹ The disorder is a consequence of the reduced production of bile acids, predominantly chenodeoxycholic acid (CDCA), and an increased formation of cholestanol.² Common clinical manifestations include infant-onset diarrhea and juvenile-onset bilateral cataract, usually followed by tendon xanthomas and progressive neurological dysfunction.³ The final diagnosis is based on biochemical abnormalities, including elevated plasma cholestanol level and increased levels of bile alcohol in urine associated with a diminished biliary concentration of CDCA.⁴ The treatment is based on oral supplementation of CDCA, which, if initiated early, can prevent major clinical problems, as it produces a reduction in cholestanol synthesis and plasma levels.³

Cardiovascular impairment in patients with CTX is mostly associated with premature atherosclerosis.⁴ Blood lipid analysis in patients with CTX revealed dramatically high levels of 27-hydroxycholesterol and low levels of high-density lipoprotein cholesterol (HDL), which place these patients at a high risk of cardiovascular disease.⁵

Spontaneous coronary artery dissection (SCAD) is defined as a non-traumatic separation of the coronary arterial wall, creating a false lumen, which leads to blood flow reduction.⁶ Although there are other systemic conditions that make the coronary vessel wall vulnerable to this condition, in patients with atherosclerotic coronary artery disease, the rupture of a thin-cap fibroatheroma might lead to SCAD.⁷

We describe a case report of a patient diagnosed with CTX who showed cardiac impairment due to SCAD.

Keywords

Xanthomatosis Cerebrotendinous; Cholesterol; Cholestanol; Chenodeoxycholic Acid/adverse effects; Diagnosis, Imaging; Child, Adolescent.

Mailing Address: Maria Julia Silveira Souto •

Universidade Federal de Sergipe – Avenida Marechal Rondon, s/n.

Postal Code 49100-000, São Cristóvão, SE – Brazil

E-mail: souto.mjulia@gmail.com

Manuscript received July 09, 2019, revised manuscript October 05, 2019, accepted September 13, 2019

DOI: <https://doi.org/10.36660/abc.20190456>

Case report

In 2013, a female patient, 22 years old, reported a history of xanthomas in the Achilles tendon and complex partial epileptic crisis for the last 10 years. She developed progressive difficulty in learning and walking skills. Associated to this clinical presentation, she reported a history of bilateral surgery for cataract when she was 14 years old and steatorrhea.

On physical examination, xanthomas were observed mostly on the region of the Achilles tendon, bilaterally, but also on the right elbow and knee (Figure 1). The neurological exam showed mild dysmetria and dysidiadochokinesia, difficulty performing the straight line walking test, and bilateral and symmetric patellar hyperreflexia. There was no abnormality on strength or sensitivity exams.

The magnetic resonance imaging of the brain showed a focal area of 1.4 cm, with hypersignal in T2-weighted and hyposignal in T1-weighted sequences, with no contrast enhancement. The transthoracic echodopplercardiogram found a moderate left ventricular dilatation and regional dysfunction, resulting in a moderate impairment in its systolic function, and a mild mitral regurgitation. The abdominal ultrasound showed cholelithiasis.

The patient, therefore, had clinical and radiological findings compatible with CTX. The diagnosis was confirmed by an elevated serum cholestanol level of 31.79 mcg/mL. She started the treatment with CDCA in the same year.

In 2017, she was submitted to a new cardiovascular examination. A cardiac magnetic resonance imaging was performed and showed a dilated left ventricle, associated with mild left ventricular dysfunction (left ventricular ejection fraction = 47%), as a consequence of akinesia of the inferior medium-basal wall and dyskinesia in the anterior and anterior-septal walls of the left ventricle. These regions showed perfusion impairment in the gadolinium-based dynamic evaluation and the presence of transmural late gadolinium enhancement (Figure 2).

The coronary computed tomographic angiography detected severe parietal irregularity in the proximal third of the anterior descending coronary artery (LAD) with luminal reduction of 50%, which suggested the presence of a noncalcified plaque or dissection of the artery (Figure 3).

The latter was confirmed by coronary angiography and intracoronary ultrasound, which showed a dissection in the medial and proximal thirds of the LAD, with no impairment of the distal flow (Figure 4).

At the time of diagnosis, her lipid panel was: total cholesterol 170 mg/dL; high-density lipoprotein cholesterol



Figure 1 – Xanthomas observed on the region of the right Achilles tendon and on the right knee.

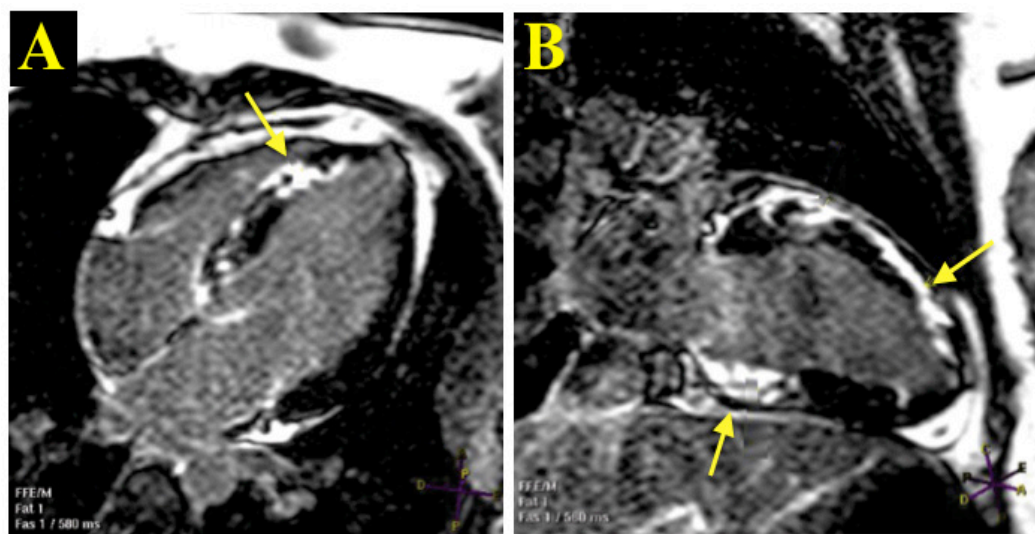


Figure 2 – Magnetic resonance imaging showing transmural late gadolinium enhancement (arrows) of the inferior medium-basal, anterior and anterior-septal walls of the left ventricle in four-chamber (A) and two-chamber views (B).

(HDL-C) 47 mg/dL; low-density lipoprotein cholesterol (LDL-C) 101 mg/dL; triglycerides 108 mg/dL.

Based on these findings, the patient was started on cardiovascular therapy with Ramipril 10 mg per day, Aspirin 100 mg per day, Carvedilol 6.25 mg twice a day and Rosuvastatin 10 mg at bedtime, associated to the maintenance of the oral bile acid supplementation with CDCA.

Discussion and Conclusions

Cerebrotendinous xanthomatosis is caused by a homozygous mutation of the mitochondrial enzyme sterol 27-hydroxylase (CYP27), which leads to a number of systemic manifestations.⁸ The diagnosis is established upon recognition of these symptoms and the finding of elevated plasma cholestanol,

and, if possible, a definitive diagnosis is obtained through the molecular analysis of CYP27A1 gene.^{9,10} In the present case, the diagnosis of CTX was established based on the strong symptomatology associated with plasma cholestanol levels, which were very similar to the mean serum concentrations found in other studies (31.79 mcg/mL).^{4,10}

Cardiac manifestations are less remarkable and present mostly as severe coronary disease, including myocardial infarction, angina pectoris, coronary artery disease and ischemic changes on the electrocardiogram.^{5,11} Subsequently, two large studies carried out by Duell et al.¹⁰ and Sekijima et al.¹² demonstrated the presence of cardiovascular disease associated to CTX only in 7% and 20% of their patients, respectively. In this case report, we studied a patient with CTX who developed coronary artery

Case Report

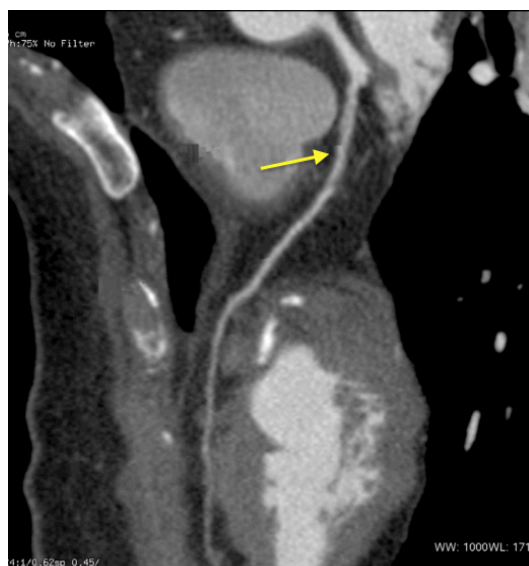


Figure 3 – Multiplanar reformation of coronary computed tomographic angiography, detecting a severe parietal irregularity in the proximal third of the anterior descending coronary artery, which suggested the presence of a noncalcified plaque or dissection of the artery (arrow).

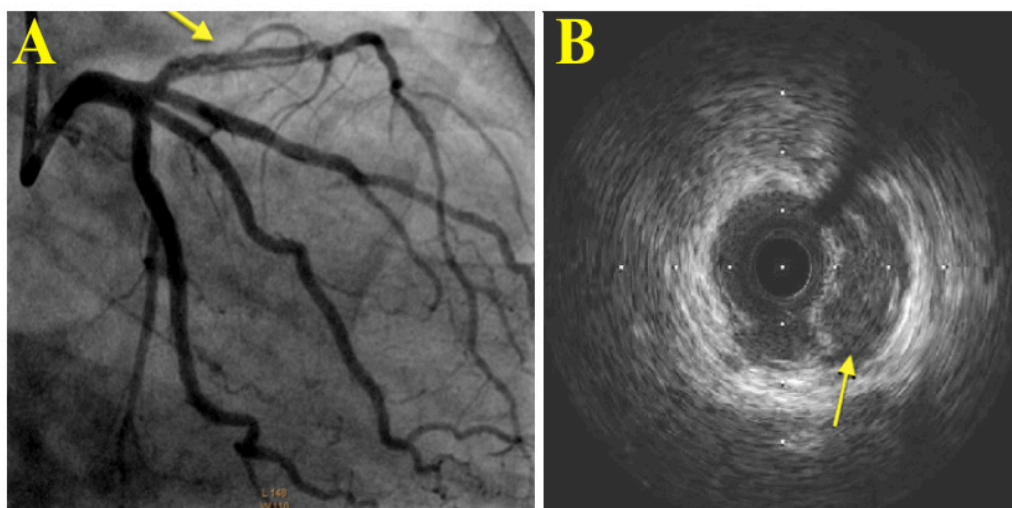


Figure 4 – A - Coronary angiography of left coronary showing dissection in the proximal and medium third of left anterior descending artery (arrow). B- Intracoronary ultrasound showing double-lumen sign in the left anterior descending artery (arrow).

disease due to SCAD. Although several specific clinical situations, including fibromuscular dysplasia and pregnancy, have been mostly associated with SCAD, atherosclerotic conditions may be as well related to the pathogenesis of this disease.⁶ As the CTX predisposes to the development of premature atherosclerosis and there are a few studies that report coronary artery disease associated to atherosclerotic thromboembolism,⁵ there is evidence that the SCAD in the reported case was also associated to an atheromatous plaque formation. As far as the authors could investigate,

this is probably the first case in the literature demonstrating the association between CTX and SCAD.

Author contributions

Conception and design of the research: Souto MJS, Sousa AC; Data acquisition: Souto MJS, Ferreira EJP, Gonçalves LFG, Sousa AC; Analysis and interpretation of the data: Souto MJS, Almeida-Santos MA, Ferreira EJP, Gonçalves LFG, Sousa AC; Writing of the manuscript: Souto MJS, Oliveira JLM,

Sousa AC; Critical revision of the manuscript for intellectual content: Almeida-Santos MA, Oliveira JLM, Sousa AC.

Potential Conflict of Interest

The authors report no conflict of interest concerning the materials and methods used in this study or the findings specified in this paper.

Sources of Funding

There was no external funding source for this study.

Study Association

This study is not associated with any thesis or dissertation.

Ethics approval and consent to participate

This study was approved by the Ethics Committee of the Universidade Federal de Sergipe under the protocol number CAAE: 0289.0.107.000-11. All the procedures in this study were in accordance with the 1975 Helsinki Declaration, updated in 2013. Informed consent was obtained from all participants included in the study.

References

1. Moghadasian MH, Salen G, Frohlich JJ, Scudamore CH. Cerebrotendinous Xanthomatosis. *Arch Neurol*. 2002;59(4):527-9.
2. Pilo-de-la-Fuente B, Jimenez-Escrig A, Lorenzo JR, Pardo J, Arias M, Ares-Luque A, et al. Cerebrotendinous xanthomatosis in Spain: clinical, prognostic, and genetic survey. *Eur J Neurol*. 2011;18(10):1203-11.
3. Tibrewal S, Duell PB, DeBarber AE, Loh AR. Cerebrotendinous xanthomatosis: early diagnosis on the basis of juvenile cataracts. *J Am Assoc Pediatr Ophthalmol Strabismus* 2017;21(3):505-7.
4. Nie S, Chen G, Cao X, Zhang Y. Cerebrotendinous xanthomatosis: a comprehensive review of pathogenesis, clinical manifestations, diagnosis, and management. *Orphanet J Rare Dis*. 2014;9(9) 1-11.
5. Passaseo I, Cacciotti L, Pauselli L, Ansalone G. Acute myocardial infarction in patient with cerebrotendinous xanthomatosis: Should these patients undergo stress tests during screening? *J Cardiovasc Med*. 2012;13(4):281-3.
6. Yip A, Saw J. Spontaneous coronary artery dissection-A review. *Cardiovasc Diagn Ther* 2015;5(1):37-48.
7. Alfonso F, Bastante T, Rivero F, Cuesta J, Benedicto A, Saw J, Gulati R. Spontaneous Coronary Artery Dissection. *Circ J* 2014;78(9):2099-110.
8. Lorincz MT, Rainier S, Thomas D, Fink JK. Cerebrotendinous Xanthomatosis. *Arch Neurol* 2005;62(9):1459-63.
9. Salen G, DeBarber A, Eichler F, Casaday L, Jayadev S, Kisanuki Y, et al. The Diagnosis and Treatment of Cerebrotendinous Xanthomatosis. *J Clin Lipidol*. 2018;12(5):545-6.
10. Duell PB, Salen G, Eichler FS, DeBarber AE, Connor SL, Casaday L, et al. Diffenderfer MR, Schaefer EJ. Diagnosis, treatment, and clinical outcomes in 43 cases with cerebrotendinous xanthomatosis. *J Clin Lipidol*. 2018;12(5):1169-78.
11. Fujiyama J, Kuriyama M, Arima S, Shibata Y, Nagata K, Takenaga S, et al. Atherogenic risk factors in cerebrotendinous xanthomatosis. *Clin Chim Acta*. 1991;200(1):1-11.
12. Sekijima Y, Koyama S, Yoshinaga T, Koinuma M, Inaba Y. Nationwide survey on cerebrotendinous xanthomatosis in Japan. *J Hum Genet*. 2018;63(3):271-80.



This is an open-access article distributed under the terms of the Creative Commons Attribution License

A Case of Acute Myocardial Infarction and Pericarditis Unmasking Metastatic Involvement of the Heart

Sofia Torres,¹^{ID} Mariana Vasconcelos,¹ Carla Sousa,¹ Antonio J. Madureira,¹^{ID} Alzira Nunes,¹^{ID} Maria Júlia Maciel¹

Centro Hospitalar Universitário de São João,¹ Porto – Portugal

Introduction

Metastases to the heart and pericardium are much more common than primary cardiac tumors and are generally associated with a poor prognosis.^{1,2} While they are most commonly asymptomatic, cardiac metastases can mimic primary cardiac diseases such as acute coronary syndromes, congestive heart failure and pericarditis.^{3,4} Lung cancer is the most frequent source of metastatic cardiac disease, either from direct extension or by a combination of lymphatic, hematogenous, and transvenous dissemination.^{2,5}

Case Report

We present a case of a 62-year-old male patient who had a medical history of hypertension and dyslipidemia and was a current smoker. He was first admitted to the hospital due to a lateral wall ST-segment elevation myocardial infarction (STEMI). Emergent coronary angiography (performed 2 hours after the onset of chest pain) revealed an 80% stenosis of the mid left anterior descending coronary artery (LAD), a total occlusion of the Dg1 (first diagonal branch of the LAD) on its ostium and a distal 70% stenosis of the left posterolateral branch of the left circumflex coronary artery (PL). Angioplasty with drug eluting stent (DES) implantation in the LAD and balloon dilatation of the Dg1 was performed. Percutaneous coronary intervention with DES implantation in the PL was conducted a few days later.

The transthoracic echocardiogram (TTE) showed preserved biventricular systolic function with anterior and lateral wall motion abnormalities. The patient remained asymptomatic afterwards and was discharged home.

Two months after discharge, the patient was readmitted due to pleuritic chest pain, abnormal ECG showing diffuse upward concave ST-segment elevation and elevated C-reactive protein (199 mg/L) and high-sensitive troponin I (2953 ng/L). The TTE exhibited preserved biventricular systolic function with the previously reported wall motion abnormalities and mild pericardial effusion. Based on this presentation, the diagnostic

hypotheses raised were Dressler syndrome versus other causes of pericarditis with associated myocardial injury.

A cardiac magnetic resonance imaging (cMRI) was performed for further evaluation, which revealed an intrapericardial elongated mass (measuring 25 x 13 x 40 mm) adjacent to the basal anterior and anterolateral segments and in close contact with the LAD stent (Figure 1). This mass had isointense signal intensity on T1-weighted images, high signal intensity on T2-weighted images, first-pass perfusion, and heterogeneous late gadolinium enhancement (LGE). Subendocardial LGE in the mid-basal anterior and anterolateral segments confirmed the previous infarction in the LAD territory. Contrast-enhanced pericardium was also noted, due to inflammatory activity.

At first, these findings raised concerns about a complication of the previous endovascular procedure involving the LAD artery, such as coronary dissection or perforation with an organizing hematoma. A new coronary angiography showed persistence of the good result regarding the LAD stent, with no signs of procedure complications. A neoplastic origin of the mass was then suspected. A thoracic computed tomography (CT) was performed and unveiled a suspicious lesion in the left hilum, just next to the left superior lobe bronchus with invasion of the left superior pulmonary vein (Figure 2). A biopsy of the left pulmonary lesion revealed a carcinoid tumor of the lung.

The presence of lymphadenopathy and pleural nodules pointed toward a metastatic nature of the mass adjacent to the LAD. High sensitive troponin elevation was interpreted as related to myocardial infiltration. Despite the presence of atherosclerotic disease in other coronary arteries, the hypothesis of external compression of the LAD by the metastatic mass as a contributor to the previous lateral wall STEMI could not be excluded.

The final diagnosis was a primary lung malignancy with secondary involvement of the heart.

Further investigation later unveiled widespread metastatic disease with bone, parotid gland, pancreatic and brain involvement and the patient started on targeted chemo- and radiotherapy. At two years of follow-up, the patient is free from cardiac symptoms and events and remains on palliative chemotherapy.

Keywords

Myocardial Infarction; Pericarditis; Cardiac metastases; Lung Neoplasms; Multimodality Imaging; Cardiac Magnetic Resonance; Computed Tomography

Mailing Address: Sofia Torres •

Hospital de São João - Alameda Prof. Hernâni Monteiro 4200-319, Porto – Portugal E-mail: sofiaacardosotorres@gmail.com
Manuscript received August 09, 2019, revised manuscript October 06, 2019, accepted October 29, 2019

DOI: <https://doi.org/10.36660/abc.20190534>

Conclusion

Symptoms related to metastatic heart disease, which can be nonspecific and mimic other cardiac disorders such as coronary artery disease or pericarditis, can rarely be the first manifestation of a previously unknown malignancy. Whereas echocardiography is the most frequently used imaging method to examine the heart and pericardium, multimodality imaging with cMRI and CT offers advantages in the diagnosis of metastatic heart disease,^{6,7} as was demonstrated in this case.

Author contributions

Case Report

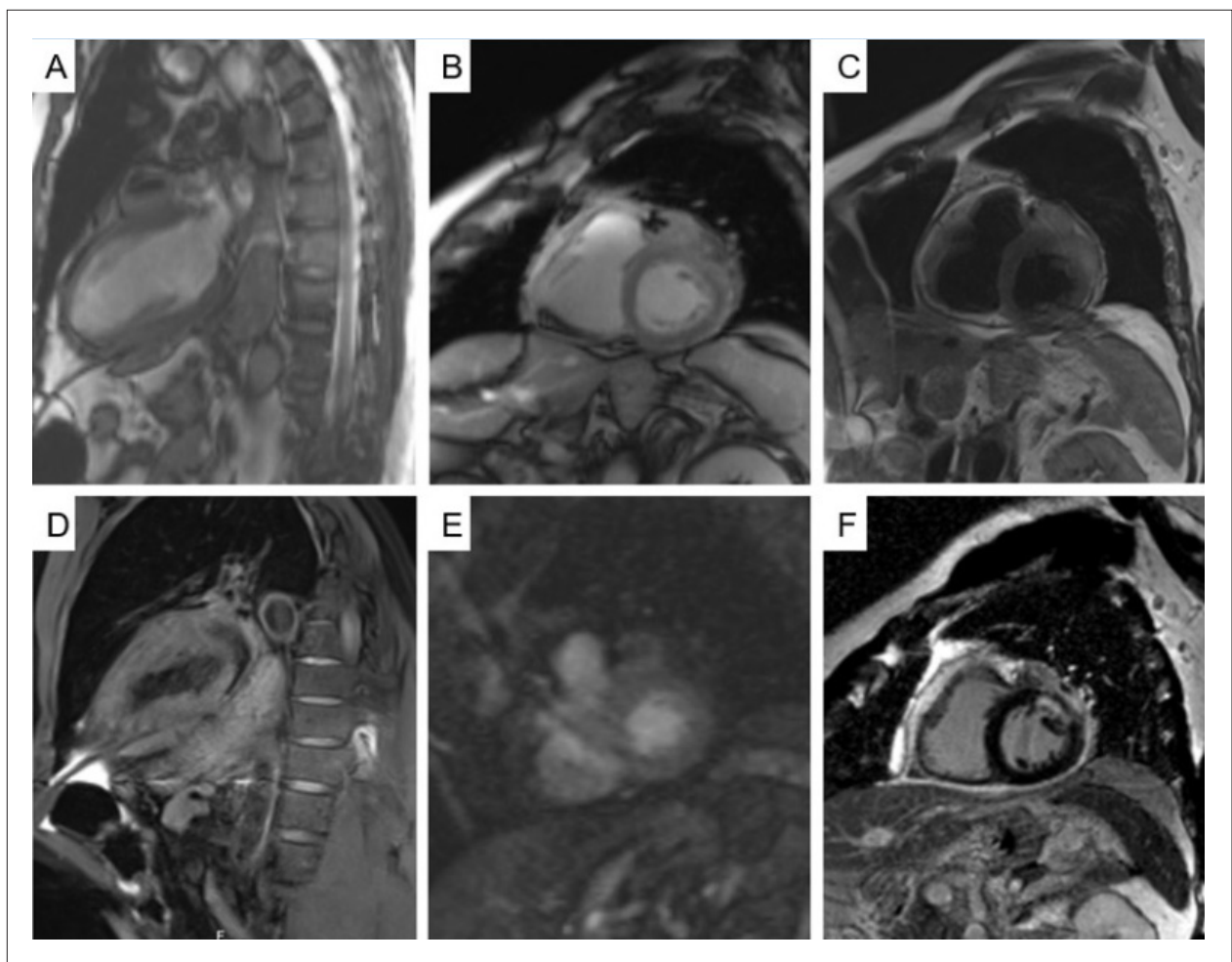


Figure 1 – cMRI (A) (B) b-SSFP cine images revealing an elongated mass (measuring 25 x 13 x 40 mm) adjacent to the basal anterior and antero-lateral segments and in close contact with the LAD artery stent. (C) High intensity signal on T2-weighted images. (D) Isointense signal intensity on T1-weighted images. (E) First pass perfusion of the mass. (F) LGE with heterogeneous appearance of the mass and diffuse contrast-enhanced pericardium.

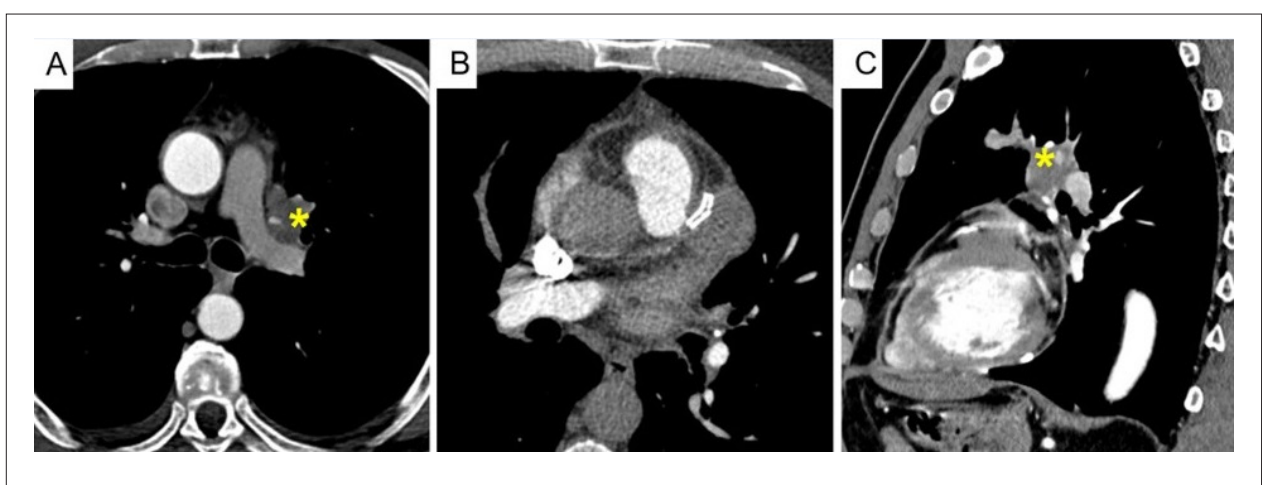


Figure 2 – Thoracic CT (A) (C) Suspicious pulmonary lesion (*) in the left hilum, just next to the left superior lobe bronchus with invasion of the left superior pulmonary vein. (B) Metastatic mass in close contact with the LAD stent causing secondary involvement of the pericardium.

Case Report

Conception and design of the research and Writing of the manuscript: Torres S; Data acquisition: Torres S, Vasconcelos M, Sousa C, Madureira AJ; Analysis and interpretation of the data: Torres S, Vasconcelos M, Sousa C, Madureira AJ; Critical revision of the manuscript for intellectual content: Vasconcelos M, Sousa C, Madureira AJ, Nunes A, Maciel MJ.

Potential Conflict of Interest

The authors report no conflict of interest concerning the materials and methods used in this study or the findings specified in this paper.

Sources of Funding

There was no external funding source for this study.

Study Association

This study is not associated with any thesis or dissertation.

Ethics approval and consent to participate

This article does not contain any studies with human participants or animals performed by any of the authors.

References

1. Ghosh AK, Crake T, Manisty C, Westwood M. Pericardial Disease in Cancer Patients. *Curr Treat Options Cardiovasc Med*. 2018; 20(7):60.
2. Hudzik B, Misalski-Jamka K, Glowacki J, Lekston A, Gierlotka M, Zembala M, et al. Malignant tumors of the heart. *Cancer Epidemiol*. 2015; 39(5):665-672.
3. Lichtenberger JP, Reynolds DA, Keung J, Keung E, Carter BW. Metastasis to the Heart: A Radiologic Approach to Diagnosis with Pathologic Correlation. *AJR Am J Roentgenol*. 2016; 207(4):764-72.
4. Burazor I, Aviel-Ronen S, Imazio M, Goitein O, Perelman M, Shelestovich N, et al. Metastatic cardiac tumors: from clinical presentation through diagnosis to treatment. *BMC Cancer*. 2018; 18(1):202.
5. Goldberg AD, Blankstein R, Padera RF. Tumors metastatic to the heart. *Circulation*. 2013; 128(16):1790-4.
6. Kassop D, Donovan MS, Cheezum MK, Nguyen BT, Gambill NB, Blankstein R, et al. Cardiac Masses on Cardiac CT: A Review. *Curr Cardiovasc Imaging Rep*. 2014; 7(8):9281.
7. Pazos-López P, Pozo E, Siqueira ME, García-Lunar I, Cham M, Jacobi A, et al. Value of CMR for the differential diagnosis of cardiac masses. *JACC Cardiovasc Imaging*. 2014; 7(9):896-905.



Este é um artigo de acesso aberto distribuído sob os termos da licença de atribuição pelo Creative Commons

A Complicated “One Segment” Myocardial Infarction: The Role of Cardiovascular Imaging

Ana Rita Pereira,¹ Ana Rita Almeida,¹ Inês Cruz,¹ Luis Rocha Lopes,^{2,3,4} Maria José Loureiro,¹ Hélder Pereira^{1,4}

Cardiology Department, Hospital Garcia de Orta EPE,¹ Almada - Portugal

Barts Heart Centre, Barts Health NHS Trust,² London - England

Institute of Cardiovascular Science, University College London,³ London - England

Cardiovascular Center, Lisbon Academic Medical Center, University of Lisbon,⁴ Lisbon - Portugal

Introduction

The incidence of mechanical complications (MC) after myocardial infarction (MI) was reduced to less than 1% with the routine use of primary reperfusion therapies.¹ MC are classified as early, including acute and subacute forms, and late or chronic.² The former mostly present as cardiogenic shock² and the latter may vary from asymptomatic to sudden death.³ As all of these conditions may have potentially lethal consequences, timely diagnosis and treatment is necessary.¹⁻³

Case Report

A 57-year-old woman with smoking habits was admitted to the Emergency Department with oppressive anterior chest pain, nausea, and vomiting. Four days earlier, the patient reported similar symptoms with hours of evolution but spontaneous relief. Upon admission, she was conscious and maintained chest pain. Medical examination revealed hypotension, tachycardia, polypnea, and signs of decreased peripheral perfusion.

A 12-lead electrocardiogram showed sinus tachycardia with a 4 mm ST-segment elevation in DI and aVL leads, and a 4 mm ST-segment depression in inferior leads. Additional work-up revealed lactic acidosis, elevated systemic inflammatory parameters, and increased myocardial necrosis markers. Transthoracic echocardiogram (TTE) demonstrated a hypertrophic and non-dilated left ventricle with lateral hypokinesia, but with preserved systolic function; a moderate pericardial effusion with partial diastolic collapse of the right cavities; and a dilated inferior vena cava without respiratory variation (Figure 1; Video 1). There were no significant valvular findings and the aortic root and arch were normal.

Due to suspicion of subacute ST-elevation myocardial infarction (STEMI) complicated by left ventricular (LV) free wall rupture (FWR), no anti-thrombotic medication was

administered, and the patient was submitted to an invasive coronary angiography (ICA) and ventriculography (Video 2). A 90% stenosis of the posterolateral branch was observed, although apparently no occlusive lesion, ventricular rupture or segmental wall motion abnormalities were found.

After angiography, her clinical status worsened. Cardiac tamponade was admitted and an emergency percutaneous pericardiocentesis was performed with drainage of 200 mL of hematic fluid with no spontaneous coagulation, resulting in global improvement (Figure 2). Fluid analysis revealed an exudate and normal adenosine deaminase. Microbiological analyses were negative and the cytological test did not reveal neoplastic cells. In order to determine the effusion aetiology, viral serologies, autoimmunity, and thoracoabdominal-pelvic computed tomography were also performed with normal results.

Given the absence of a specific diagnosis, a cardiac magnetic resonance imaging (CMR) was performed eight days after hospital admission. It revealed dyskinesia of the mid-segment of the lateral wall in the cine sequences, transmural hyperintense sign in the T2-weighted short-tau inversion recovery images (Figure 3A and 3B) — compatible with oedema — and late transmural enhancement (Figure 3C and 3D) — suggesting myocardial necrosis — of this segment. These findings were compatible with subacute MI of the mid-segment of the lateral wall with no apparent viability. Moreover, the absence of myocardial tissue between the mid-segments of the lateral and inferolateral walls was observed, surrounded by a small saccular protuberance with a narrow neck, suggesting a pseudoaneurysm at that location (Figure 3E and 3F; Video 3).

Thus, the initially suspected diagnosis was confirmed: subacute STEMI complicated with LV FWR that evolved to cardiac tamponade and posteriorly to a pseudoaneurysm formation. Due to the risk of fatal complications, the patient was submitted to cardiac surgery. With no need for cardiopulmonary bypass, a coronary artery bypass grafting with saphenous vein graft to the posterolateral artery and a pseudoaneurysm plication were performed. Currently, she is asymptomatic.

Discussion

FWR is an uncommon and early MC of MI, with a reported incidence of less than 1%.² There are two clinical groups: the “blow-out type” (complete or acute rupture) with a macroscopic defect and high-volume bleeding, leading to cardiac tamponade; and the “oozing type” (incomplete or subacute rupture) without an obvious bleeding source and

Keywords

Heart Rupture; Myocardial Infarction; Aneurysm, False; Diagnostic, Imaging; Echocardiography/methods.

Mailing Address: Ana Rita F. Pereira •

Hospital Garcia de Orta EPE – Cardiologia - Avenida Torrado da Silva Almada, 2805-267 – Portugal

E-mail: pereira.anarita@gmail.com

Manuscript received May 17, 2019, revised manuscript September 16, 2019, accepted October 23, 2019

DOI: <https://doi.org/10.36660/abc.20190323>

Case Report

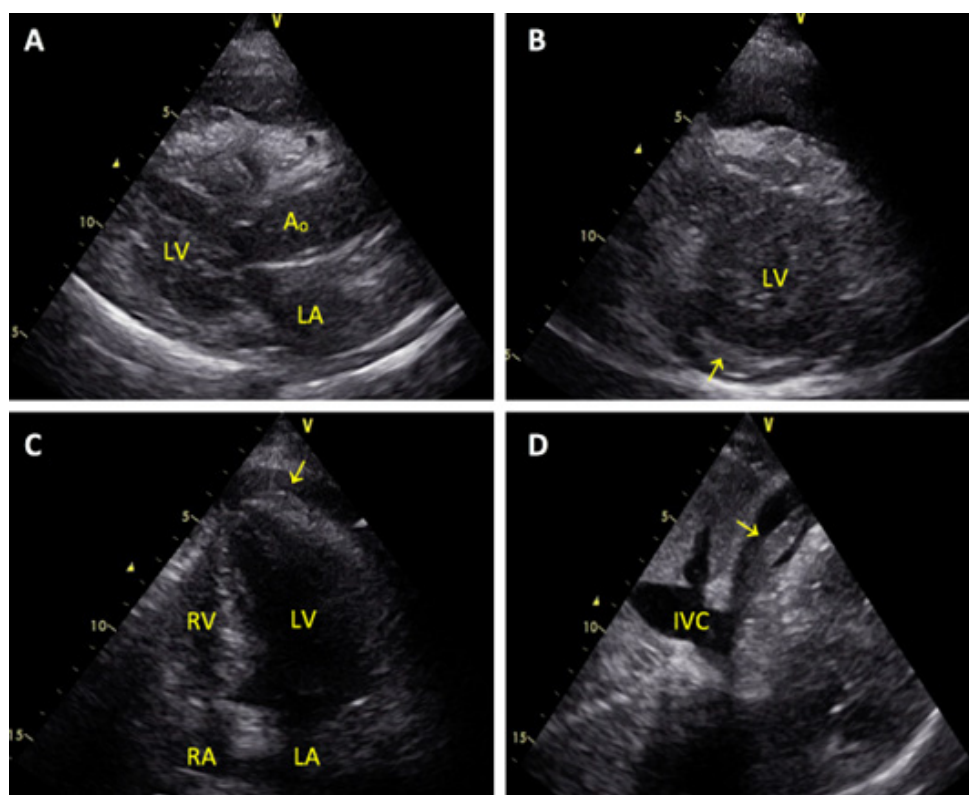


Figure 1 – Transthoracic echocardiogram. (A) Parasternal long-axis and (B) Parasternal short-axis views showing a mild hypertrophic and non-dilated left ventricle; (C) Apical 4-chamber view showing a partial collapse of right cavities and a lateral hypokinesia but preserved systolic function of the left ventricle; (D) Subcostal view showing a dilated inferior vena cava, with no respiratory size variation. The yellow arrow indicates a moderate pericardial effusion. LV: left ventricle; LA: left atrium; Ao: Ascending aorta; RV: right ventricle; RA: right atrium; IVC: inferior vena cava



Figure 2 – Drainage system of percutaneous pericardiocentesis with around 200 mL of hematic pericardial fluid.

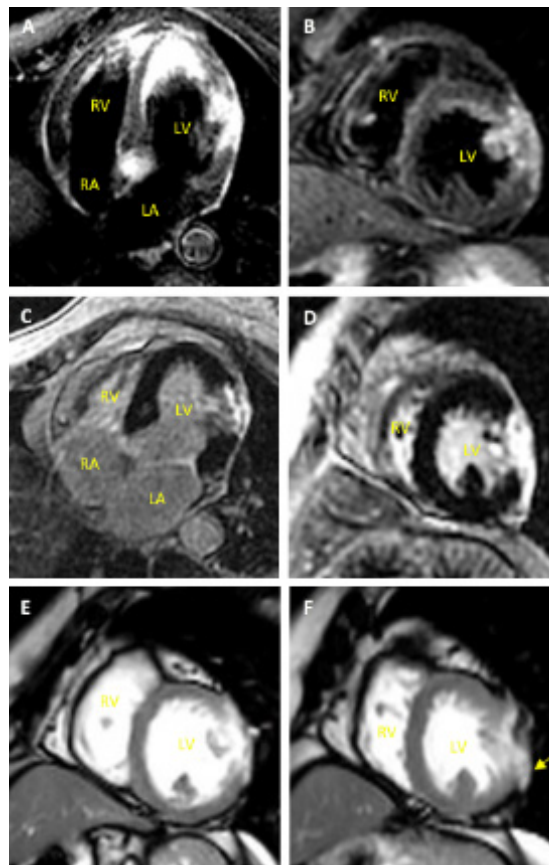


Figure 3 – Cardiac magnetic resonance imaging. (A) Four-chamber and (B) short-axis views, T2-weighted short-tau inversion recovery (STIR) images, showing transmural hyperintense sign of the mid-segment of the lateral wall compatible with oedema; (C) Four-chamber and (D) short-axis views, late gadolinium enhancement images, showing contrast enhancement of the same segment, suggesting myocardial necrosis; (E) End-diastolic and (F) end-systolic phases, steady-state free precession (SSFP) cine images, showing dyskinesia of the mid-segment of lateral wall and a saccular protuberance suggesting a pseudoaneurysm (yellow arrow).

slow blood accumulation.² The latter type corresponds to up to one-third of the cases and can progress to complete rupture or pseudoaneurysm formation.¹⁻³ In both types, immediate surgery is vital, as FWR has a mortality rate ranging between 60 and 96%.⁴

LV pseudoaneurysm formation is an even rarer MC, with a reported prevalence of 0.05%.^{5,6} It is a late consequence of an undiscovered or unoperated LV FWR, formed when the myocardial rupture is contained by an adherent layer of pericardium, scar tissue or clot formation.² As a result, the initial event is typically self-limited and bleeding causes an hemopericardium not manifested by cardiac tamponade.² Urgent surgery is indicated as untreated pseudoaneurysms have a 30 to 45% risk of rupture and a mortality rate of 50%.^{3,5}

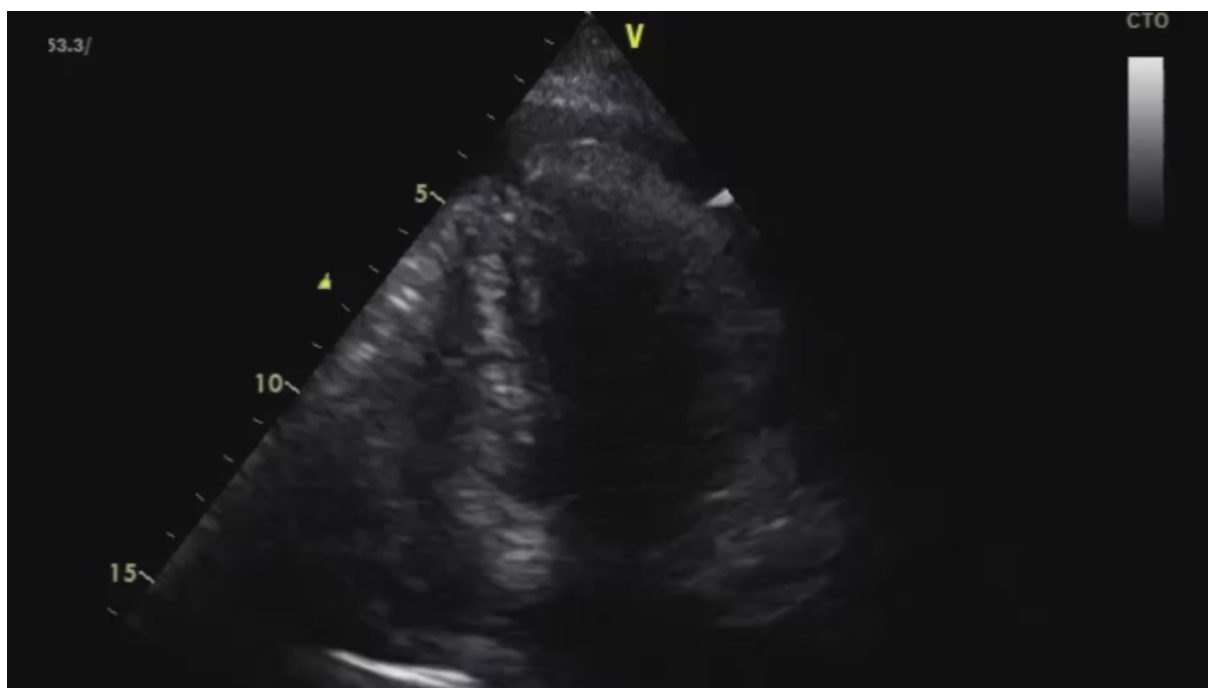
In the reported clinical case, an atypical form of incomplete or subacute LV FWR resulting in both cardiac tamponade and pseudoaneurysm formation was described.

Concerning diagnosis, TTE is the cornerstone for the initial evaluation of MC following MI.² Pericardial effusion is the main echocardiographic finding in LV FWR.⁷ However, in cases of pseudoaneurysm, TTE is diagnostic in only 26% of

patients and the gold standard method, for its identification is ventriculography.⁸ When pseudoaneurysm diagnosis cannot be established by any of the previous methods, CMR is a reliable alternative, as illustrated by the presented case report. It accurately identifies pseudoaneurysms and distinguishes them from true aneurysms.⁹⁻¹¹ Pseudoaneurysms, or false aneurysms, commonly involve lateral or inferior walls; they have no myocardial elements and are characterized by a narrow neck (ratio of the maximum diameter of the orifice to the maximum internal diameter of the cavity of 0.25-0.5) and an abrupt transition from normal myocardium to the defect.⁹⁻¹¹ True aneurysms are more common in apical, anterior or anterolateral locations; contain elements of myocardium and include a wide neck (diameters ratio of 0.9-1.0) and a smooth transition from normal to thinned myocardium.⁹⁻¹¹ The previous differentiating features presented in the CMR were crucial for the final diagnosis of our patient.

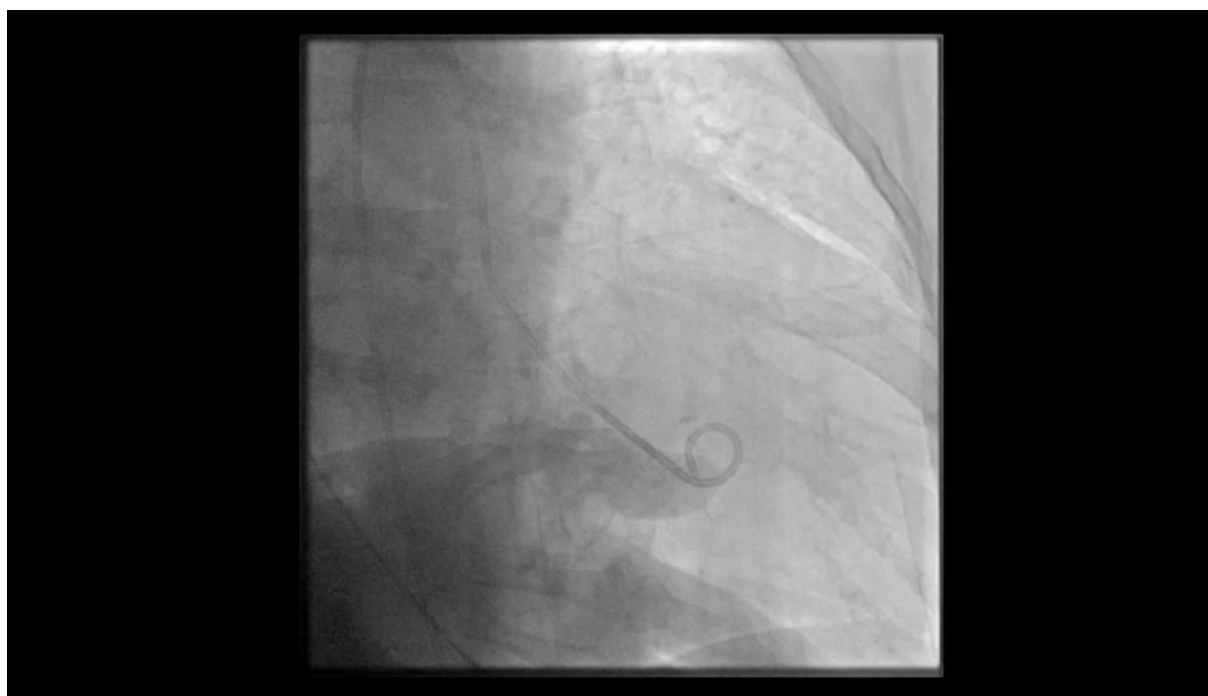
Emergency pericardiocentesis also enables the diagnosis of the LV FWR, when an hemopericardium is present. In these cases, spontaneous coagulation of pericardial fluid is usually observed, due to the overwhelming of the fibrinolytic

Case Report



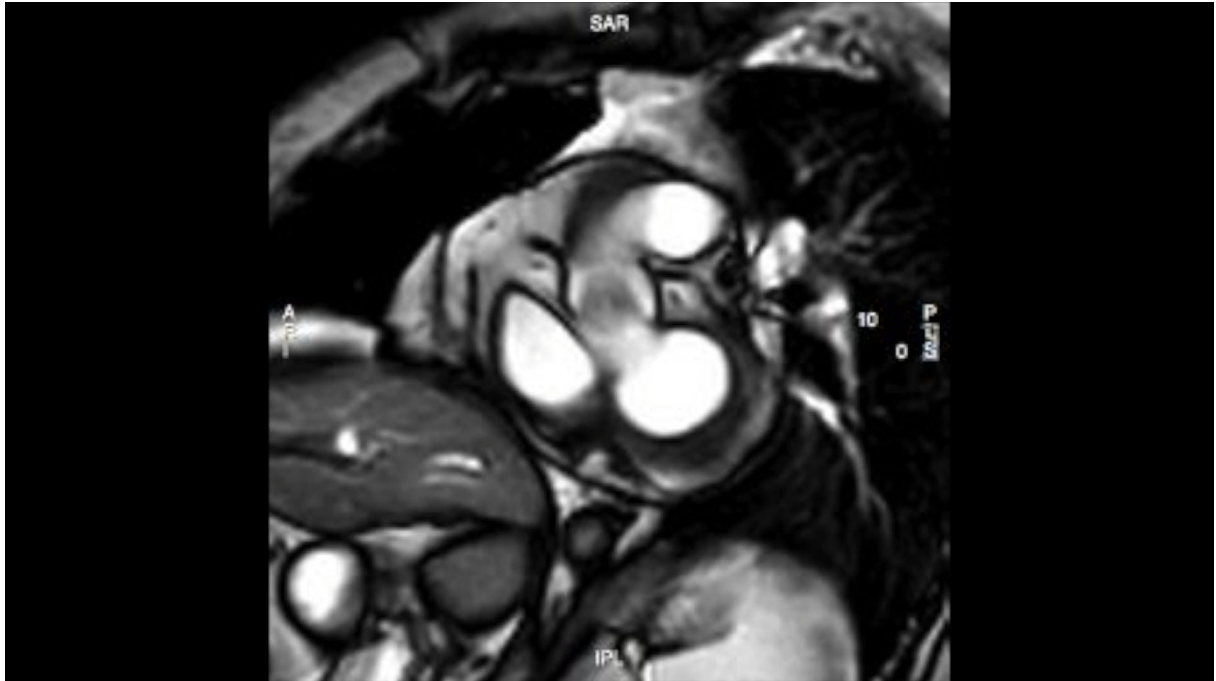
Video 1 – Transthoracic echocardiogram, four-chamber view, showing a non-dilated left ventricle with lateral hypokinesia and a moderate pericardial effusion with partial diastolic collapse of right cavities.

Access the video here: <https://bit.ly/2YAoPYU>



Video 2 – Ventriculography showing no apparent ventricular rupture or segmental wall motion abnormalities.

Access the video here: <https://bit.ly/2YAoPYU>



Video 3 – Cardiac magnetic resonance imaging, steady-state free precession cine images, sequentially short-axis, four-chamber and three-chamber views, showing dyskinesia of the mid-segment of the lateral wall and a saccular protuberance between the mid-segments of the lateral and inferolateral walls, suggesting a pseudoaneurysm. Access the video here: <https://bit.ly/2YAoPYU>

and anticlotting activities of the pericardial mesothelium.¹² Its absence does not exclude the diagnosis, but other causes must be considered,¹² as illustrated by the reported clinical case.

Finally, no immediate reperfusion therapy was performed on this patient, since ICA did not show any apparent occlusive lesion. Hemodynamic stabilization was the priority. Later, despite the lack of viability of the involved segment demonstrated by CMR, the posterolateral branch was revascularized as it was considered responsible for perfusion of non-necrotic segments.

Conclusion

This clinical case demonstrates an extremely rare MC following MI: an atypical form of incomplete or subacute LV FWR resulting in both cardiac tamponade and pseudoaneurysm formation. It also illustrates how difficult it can be to establish the differential diagnosis of chest pain with hemodynamic instability, and the etiology of a cardiac tamponade. Ultimately, it highlights the versatility and increasing applicability of CMR.

Author Contributions

Conception and design of the research, Data acquisition and Writing of the manuscript: Pereira AR; Critical revision of the manuscript for intellectual content: Almeida AR, Cruz I, Lopes LR, Loureiro MJ, Pereira H.

Potential Conflict of Interest

The authors report no conflict of interest concerning the materials and methods used in this study or the findings specified in this paper.

Sources of Funding

There was no external funding source for this study.

Study Association

This study is not associated with any thesis or dissertation.

Ethics Approval and Consent to Participate

This article does not contain any studies with human participants or animals performed by any of the authors.

Case Report

References

1. Magalhães P, Mateus P, Carvalho S, Leão S, Cordeiro F, Moreira JJ, et al. Relationship between treatment delay and type of reperfusion therapy and mechanical complications of acute myocardial infarction. *Eur Heart J Acute Cardiovasc Care*. 2016;5(5):468-74.
2. Durko AP, Budde RP, Geleijnse ML, Kappetein AR. Recognition, assessment and management of the mechanical complications of acute myocardial infarction. *Heart*. 2017;104(14):1216-23.
3. Yeo TC, Malouf JF, Oh JK, Seward JB. Clinical profile and outcome in 52 patients with cardiac pseudoaneurysm. *Ann Intern Med*. 1998;128(4):299-305.
4. Slater J, Brown RJ, Antonelli TA, Menon V, Boland J, Col J, et al. Cardiogenic shock due to cardiac free-wall rupture or tamponade after acute myocardial infarction: a report from the SHOCK Trial Registry. *J Am Coll Cardiol*. 2000;36(3 Suppl A):1117-22.
5. Frances C, Romero A, Grady D. Left ventricular pseudoaneurysm. *J Am Coll Cardiol*. 1998;32(3):557-61.
6. Yip HK, Wu CJ, Chang HW, Wang CP, Cheng CI, Chua S, et al. Cardiac rupture complicating acute myocardial infarction in the direct percutaneous coronary intervention reperfusion era. *Chest*. 2003;124(2):565-571.
7. Mittle S, Makaryus AN, Mangion J. Role of contrast echocardiography in the assessment of myocardial rupture. *Echocardiography*. 2003;20(1):77-81.
8. al-Saadon K, Walley VM, Green M, Beanlands DS. Angiographic diagnosis of true and false LV aneurysms after inferior wall myocardial infarction. *Cathet Cardiovasc Diagn*. 1995;35(3):266-9.
9. Marra MT, Lima JA, Illiceto S. MRI in acute myocardial infarction. *Eur Heart J*. 2011;32(3):284-93.
10. Hulten EA, Blankstein R. Pseudoaneurysms of the heart. *Circulation*. 2012;125(15):1920-5.
11. Sharma A, Kumar S. Overview of left ventricular outpouchings on cardiac magnetic resonance imaging. *Cardiovasc Diagn Ther*. 2015;5(6):464-70.
12. Spodick DH. Bloody pericardial effusion – Clinically significant without intrinsic diagnostic specificity. *Chest*. 1999;116(6):1506-7.



This is an open-access article distributed under the terms of the Creative Commons Attribution License

Case 4/2020 – Prolonged Time (38 Days) of Bilateral Pleural Effusion after Cavopulmonary Surgery, Relieved by Embolization of Systemic-Pulmonary Collateral Vessels, in a 40-Month-Old Child with Complex Heart Disease

Edmar Atik,¹ Raul Arrieta, Fernando Antibas Atik

Hospital Sírio Libanês de São Paulo, São Paulo, SP – Brazil

Clinical Data

The fetal diagnosis of complex cardiac anomaly (Double-outlet right ventricle, severe pulmonary stenosis due to anterior deviation of the infundibular septum, trabecular interventricular septal defect and hypoplasia of the left ventricle and mitral valve) was confirmed shortly after birth with severe hypoxia, relieved by prostaglandin E1 administration and dilation of the ductus arteriosus by percutaneous stent. With the recurrence of more severe hypoxia, the bidirectional Glenn operation was performed at 9 months of age. Good patient evolution was observed up to 39 months, when total cavopulmonary (Fontan) operation was performed due to the recurrence of hypoxia with 70% oxygen saturation. The patient received propranolol and ASA up to the last intervention.

Physical examination: good general status, eupneic, marked cyanosis, normal pulses in the 4 limbs. Weight: 16.35 Kgs, Height: 91 cm, BP: 90 x 60 mm Hg, HR: 116 bpm, O₂ Sat: 70%, Hg = 15.5 g, Hct = 55%.

Precordium: nonpalpable ictus cordis, without systolic impulses. Muffled heart sounds, without murmurs. Nonpalpable liver. Clear lungs.

Complementary Examinations

Electrocardiogram: Sinus rhythm, with right ventricular overload.

Chest x-ray: Cardiac area was normal with a cardiothoracic index of 0.47. The pulmonary vascular network was normal. (Figure 1).

Echocardiogram: *situs solitus* in levocardia, concordant atrioventricular connection and Double-outlet right ventricle connected with the anterior aorta, large interatrial septal defect, unrelated trabecular interventricular septal defect, measuring 8 mm in diameter and 4 mm effective area due to subvalvular tissue protrusion causing turbulent flow and

with a 22 mmHg interventricular pressure gradient, normal tricuspid valve and dysplastic mitral valve with thickened and redundant leaflets. The mitral valve chordae tendineae passed through the ventricular septal defect (VSD) towards the pulmonary subvalvular region. The pulmonary valve was thick and small, without anterograde flow, with functional atresia. The aortic valve had a good opening and measured 16 mm, while the ascending aorta measured 17 mm. The right ventricle measured 22 mm and the wall hypertrophy was 7 mm. Biventricular contractility was normal.

Cardiac Catheterization: It showed similar pressures (10 mm Hg) in the superior vena cava and the pulmonary arterial tree. The pressure in the atria was 5 mmHg. Angiography in the innominate vein highlighted, in addition to the good connection of the superior vena cava in the right pulmonary artery, a well-developed pulmonary tree without obstructions. The venous return through the pulmonary veins showed good ventricular contractility and well-defined cardiac anomaly.

Clinical Diagnosis: Double-outlet right ventricle, severe pulmonary stenosis due to anterior deviation of the infundibular septum, trabecular interventricular septal defect and hypoplasia of the left ventricle and mitral valve, with bidirectional Glenn and marked hypoxia.

Clinical Reasoning: There were clinical elements leading to an arterial malposition diagnosis due to the markedly muffled heart sounds. Marked pulmonary stenosis was made evident by the absence of heart murmurs. There was no clinical evidence for the diagnosis of left ventricular hypoplasia because the functional dynamics behaved as in the situation of double outlet right ventricle with interventricular septal defect and pulmonary stenosis. The diagnosis was well established by the echocardiography.

Differential Diagnosis: In a hypoxic patient without significant murmur and with muffled heart sounds, a wide range of anomalies are included in the differential diagnosis. The main ones are the transposition of the great arteries, a single right or left ventricle and pulmonary atresia with interventricular septal defect. The diagnosis in these circumstances is always established by echocardiographic images.

Conducts: It was known from birth that the most adequate approach would be directed at total cavopulmonary surgery, which became necessary given the progression of hypoxia from the age of three. Preliminary data before the functional corrective surgery presumed a good later evolution. However, the patient evolution showed exaggerated bilateral pleural effusion that lasted 38 days, despite treatment with albumin

Keywords

Heart Defects, Congenital/cirurgia; Fontan Procedure; Double Outlet Right Ventricle; . Heart Septal Defects, Ventricular; Pulmonary Valve Stenosis.

Mailing Address: Edmar Atik •

Private clinic. Rua Dona Adma Jafet, 74, conj.73, Bela Vista.

Postal Code 01308-050, São Paulo, SP – Brazil

E-mail: conatik@incor.usp.br

DOI: <https://doi.org/10.36660/abc.20190488>

Clinicoradiological Correlation

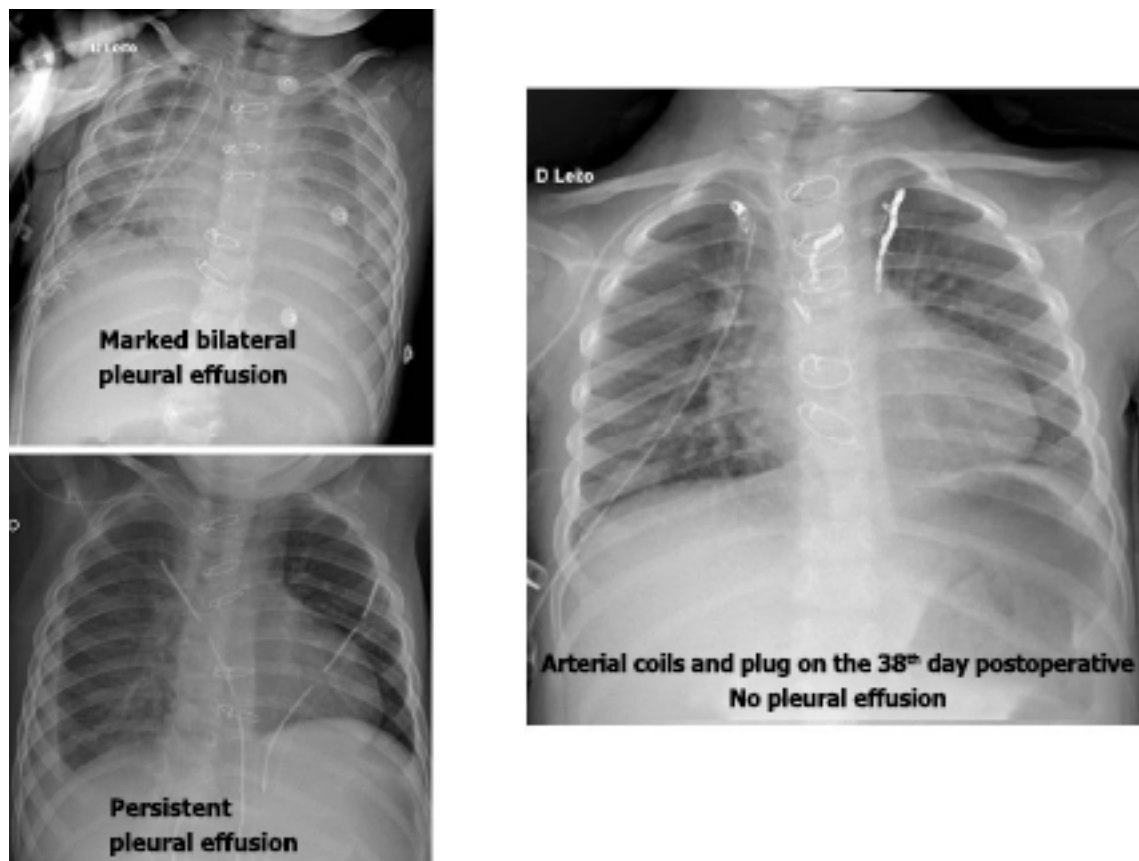


Figure 1 – Chest x-rays in the postoperative period of cavopulmonary surgery in complex heart disease. The two images on the left depict the pleural effusions and the one on the right shows after the placement of arterial coils and plug in the demonstration of the normal and hypertrophic cardiac area.

(6 to 8 g / kg / day), furosemide (4 mg / kg / day), sildenafil (3 mg / kg / day), spironolactone (2 mg / kg / day) and water restriction. The bilateral pleural effusion was exaggerated and corresponded to a volume of 300 to 500 mL per day, in a persistent manner. Due to infection in pleural fluids, the patient received antibiotics that did not solve the persistent problem. On the 34th postoperative day, cardiac catheterization was performed. The mean pulmonary pressure was 16 mmHg. In the arterial angiography, 4 discrete points of systemic-pulmonary vessels' connection were detected, sparsely distributed in the 2 lungs, coming from the internal thoracic arteries and the descending aorta. They did not cause increased saturation in the pulmonary arteries, but they were still closed by coils and an Amplatzer arterial plug (Figure 2). Four days after the interventionist catheterization, the interruption of pleural drainages was observed, followed by the consequent removal of chest drains on the 39th postoperative day. The patient was discharged on the 41st postoperative day.

Comments: The postoperative evolution of the cavopulmonary operation has many surprises, even in patients with all the adequate parameters of ventricular function, size of the pulmonary arteries, pulmonary pressure and resistance, among the main ones. The formation of systemic-pulmonary fistulas seems to occur almost immediately due to the difference in pressures that are established between arterial systems. Even if they do not seem so exuberant, their embolization is necessary, especially when the pleural effusion is persistent and there is no other evident cause. In this case, the long post-operative time that allowed for the expected accommodation of the pulmonary flow in the context of its arterial and venous tree counts as another favorable factor. The literature shows no cases with a longer duration of pleural effusion. Other procedures in similar cases include fenestration, pleurodesis, thoracic duct ligation and Fontan takedown^{1,2}.

Clinicoradiological Correlation

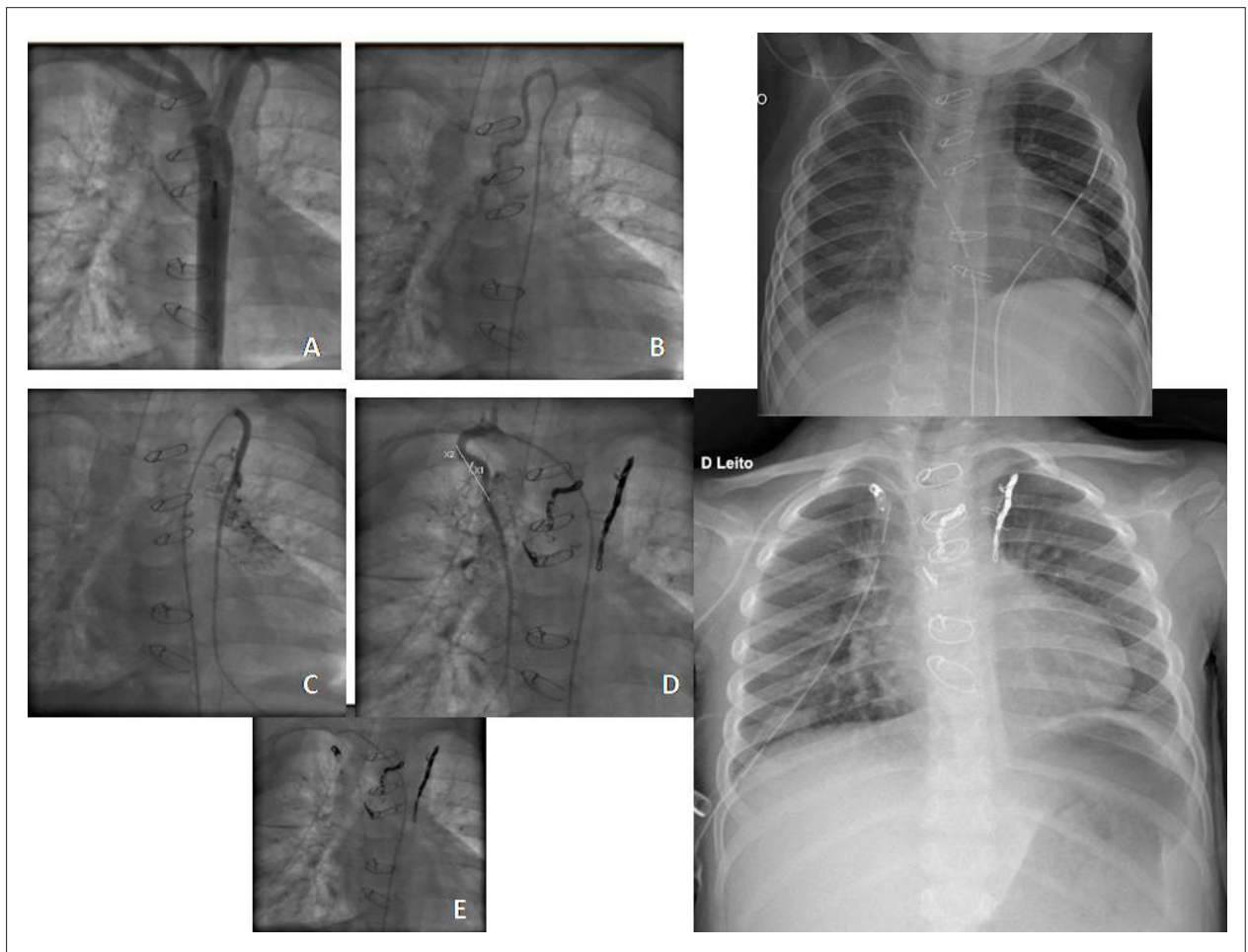


Figure 2 – Placement of arterial coils and plug for the closure of systemic-pulmonary vessels on the 38th postoperative day of the cavopulmonary surgery. In A, the fistula from the descending aorta to the right lung, in B and D from the right internal thoracic artery to the right lung, and in C, from the left thoracic artery to the left lung and in E, the arterial coils and plug after the entire procedure. The previous chest x-rays (with pleural effusion) and subsequent one (without pleural effusion), after the procedures.

References

1. Salam S, Dominguez T, Tsang V, Giardini A. Longer hospital stay after Fontan completion in the November to March period. *Eur J Cardiothorac Surg.* 2015;47(2):262-8.
2. Iyengar AJ, Winlaw DS, Galati JC, Celermajer DS, Wheaton GR, Gentles TL, et al. Trends in Fontan surgery and risk factors for early adverse outcomes after Fontan surgery: the Australia and New Zealand Fontan Registry experience. *J Thorac Cardiovasc Surg.* 2014;148(2):566-75.



This is an open-access article distributed under the terms of the Creative Commons Attribution License

Case 5/2020 – Corrected Transposition of the Great Arteries, with Good Natural Evolution in a 65-Year-Old Woman

Edmar Atik,¹ Renato Maluf Auge,¹ Alessandra Costa Barreto,¹ Maria Angélica Binotto¹

Instituto do Coração do Hospital das Clínicas da Faculdade de Medicina da Universidade de São Paulo,¹ São Paulo, SP – Brazil

Clinical data

The patient evolved without symptoms, doing her usual activities of daily living, such as housekeeping and dressmaking, when total atrioventricular block was identified during a routine evaluation with a heart rate of 66 bpm. At this time, a diagnosis of corrected transposition of the great arteries was made through the echocardiogram, with mild left atrioventricular valve regurgitation. Due to insufficient chronotropism and binodal disease, an atrioventricular pacemaker was placed on the right when she was 59 years old. She remained asymptomatic using antihypertensive medication, amlodipine, enalapril and hydrochlorothiazide. She denied any symptoms such as palpitations, chest pain or fatigue.

Physical examination: good overall status, eupneic, acyanotic, normal pulses in the four limbs. Weight: 61 Kgs, Height: 147 cm, BP=118x70 mmHg; 118 x 70 mm Hg, HR: 72 bpm.

Precordium: apical impulse on the left hemiclavicular line and somewhat impulsive, without systolic impulses on the left sternal border. Hyperphonic heart sounds, with splitting of the second sound. Mild systolic murmur +/+ +/4, more audible at the cardiac apex. Scar in the left infraclavicular region by the pacemaker implantation. Nonpalpable liver and clear lungs.

Complementary examinations

Electrocardiogram: Cardiac rhythm controlled by a pacemaker in the right atrium and signs of right bundle-branch block due to pacemaker implantation on the right at the level of the anatomically left ventricle (Figure 1).

Chest X-ray: Mild to moderate increase in the cardiac area due to an elongated left ventricular arch (CTI = 0.68). Increased pulmonary vascular network with aortic arch on the left (Figure 1).

Echocardiogram: Discordant atrioventricular and ventriculoarterial connections. Dysplastic and redundant tricuspid valve on the left. Slight enlargement of the left atrium (46 mm with volume = 36 mL/m²), and of the

right ventricle on the left, whereas the other cavities were normal (RV=44, LV=31, Ao=36 mm), as well as the other heart valves. There was no myocardial hypertrophy with septum and posterior wall = 8 mm. The pulmonary artery systolic pressure was estimated by Doppler at 26 mm Hg. Biventricular function was normal, and the left ventricular ejection fraction was 60%. RV TAPSE = 1.6 cm and RV FAC = 40%. (figure 2).

Radioisotope ventriculography: normal biventricular function (RV = 55% and LV = 53%).

Clinical Diagnosis: Corrected transposition of the great arteries with left atrioventricular valve regurgitation, of mild to moderate intensity, and total atrioventricular block showing natural evolution in an asymptomatic 65-year-old patient, with myocardial function preservation. An atrioventricular pacemaker was implanted on the right at 59 years of age.

Clinical Reasoning: There were clinical elements that led to a diagnosis of congenital heart disease, despite the absence of evident symptoms. The second hyperphonic sound in the expression of the transposition of the great arteries and the systolic murmur at the apex related to the atrioventricular valve regurgitation on the left would be the two diagnostic elements of the congenital anomaly. Moreover, there was a natural evolution to total atrioventricular block during patient evolution as an element that also led to the diagnosis. Another element would be extracted from the ECG with inverse potentials of ventricular depolarization and repolarization, but these are not available. This intricate clinical diagnosis could be performed prior to the pacemaker placement due to the lack of symptoms, but also due to the lack of a semiological clinical examination adequately performed and evaluated with adequate accuracy. The diagnosis in this case was established by the echocardiogram.

Differential diagnosis: Other cardiopathies that are accompanied by a hyperphonic second sound and systolic murmur without significance could lead to heart disease in adults that are accompanied by systemic arterial hypertension. Among the cardiopathies, one might recall the ones that, when operated, preserve the anatomy of arterial transposition, as in the transposition of the great arteries submitted to Senning's operation, as well as those operated using the total cavopulmonary technique.

Conduct: Considering the patient's good evolution in the preservation of good right ventricular function and with no significant heart defects, the expectant conduct is easily adopted, with the adequate controls of the pacemaker implanted approximately 6 years ago. Hence, the good evolution is expected to continue for many years to come.

Comments: The corrected transposition of the great arteries (CTGA) presents itself in a different way when

Keywords

Atrioventricular Block; Ventricular Dysfunction; Congenitally Corrected Transposition of the Great Arteries/surgery; Pacemaker Artificial; Adult; Diagnostic Imaging.

Mailing Address: Edmar Atik •

Private office. Rua Dona Adma Jafet, 74, conj.73, Bela Vista. Postal Code 01308-050, São Paulo, SP – Brazil
E-mail: conatik@incor.usp.br

DOI: <https://doi.org/10.36660/abc.20190489>

Clinicoradiological Correlation

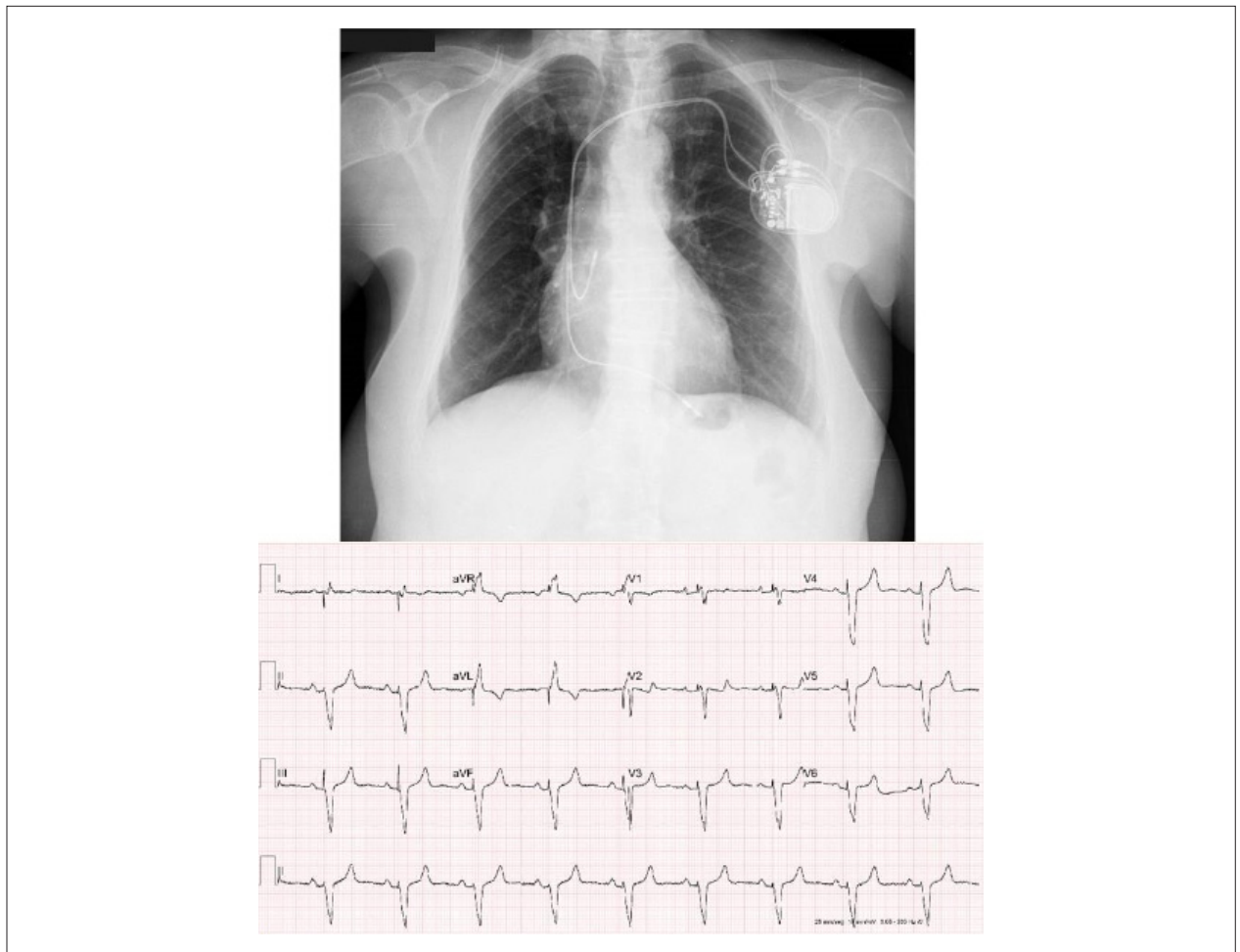


Figure 1 – Chest radiography highlights the slightly enlarged cardiac area due to a more prominent left ventricular arch and normal pulmonary vascular network. The aortic arch is located on the left. The electrocardiogram shows the good right atrioventricular pacemaker functionality, with right bundle-branch block and positioned in the left ventricle on the right.

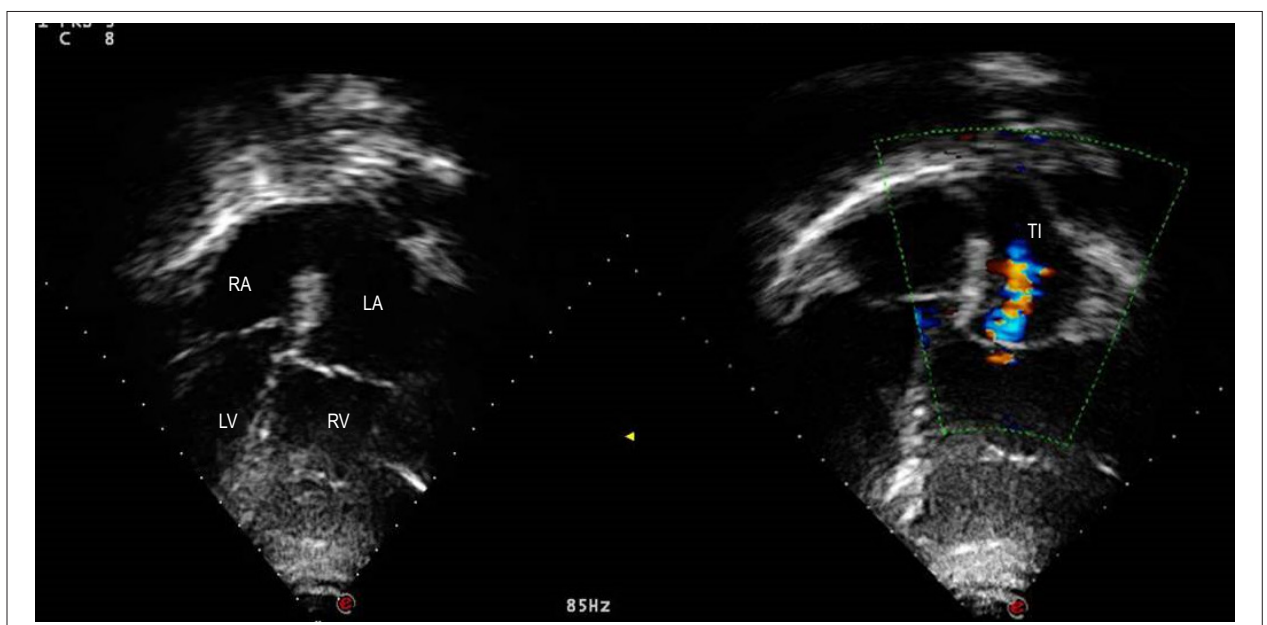


Figure 2 – Echocardiogram shows the characteristic images of corrected transposition of the great arteries with slight right ventricle dilation on the left and mild tricuspid valve regurgitation on the left. The mitral valve on the right is upper and the tricuspid valve is lower, on the left.

Clinicoradiological Correlation

externalized with associated defects in relation to their absence. It simulates Tetralogy of Fallot when it is associated with interventricular septal defect and pulmonary stenosis, VSD in the presence of the same associated defect and mitral valve regurgitation in the presence of left atrioventricular valve regurgitation. When CTGA shows no associated defects (15% of cases), the natural evolution is characterized by the evolution of the atrioventricular conduction disorder, altered by the very long right bundle, which favors the appearance of total atrioventricular block. Moreover, due to the emergence of the right ventricular insufficiency, which, due to hypertrophy and dilation, leads to relative coronary insufficiency with fibrosis and consequent ventricular

dysfunction. However, rare cases have a more favorable evolution, as in the case discussed here.

In the literature, some of these cases have also shown such a favorable evolution, citing eight of them recently described with little clinical manifestation¹. In addition to these, the oldest one was described at 83 years old and asymptomatic² and yet another patient at 70 years old, asymptomatic and with associated pulmonary valve stenosis, with a protective gradient of 49.9 mmHg between the left ventricle and the pulmonary trunk³. The management of these patients depends on the presence of symptoms, the degree of ventricular dysfunction and the complications related to the natural evolution of the congenital defect⁴.

References

1. Agarwal A, Samad F, Kalvin L, Bush M, Tajik AJ. A great imitator in adult cardiology practice: congenitally corrected transposition of the great arteries. *Congenit Heart Dis*. 2017;12(2):143-52.
2. Placci A, Lovato L, Bonvicini M. Congenitally corrected transposition of the great arteries in an 83-year-old asymptomatic patient: description and literature review. *BMJ Case Rep*. 2014 Oct 21;2014:cr2014204228.
3. Shahab H, Ashiqali S, Atiq M. Congenitally Corrected Transposition of the Great Arteries in a Septuagenarian from the Developing Country of Pakistan. *Cureus*. 2018;10(6):e2737.
4. Connolly HM, Miranda WR, Egbe AC, Warnes CA. Management of the Adult Patient With Congenitally Corrected Transposition: Challenges and Uncertainties. *Semin Thorac Cardiovasc Surg Pediatr Card Surg Annu*. 2019;22:61-5.



This is an open-access article distributed under the terms of the Creative Commons Attribution License

Case 6/2020 – 16-Year-Old Adolescent with Severe Pulmonary Stenosis At Valvar Level, After Correction of *Truncus Arteriosus* using the Barbero-Marcial Technique in the First Month of Life

Edmar Atik[®] and Miguel Barbero-Marcial

Dr Edmar Atik private clinic

Clinical Data

The newborn, in heart failure with *truncus arteriosus* type I, underwent repair at 15 days of age, weighing 2800 g. of body weight, by the Barbero-Marcial technique. At that time, the right ventricular outflow tract was approached directly with the pulmonary trunk and a monocusp valve was placed in the pulmonary position.

The evolution was adequate, with heart failure control, and he remained asymptomatic and showed normal physical development. The clinical examination ruled out residual lesions, such as pulmonary valve insufficiency. Over time, while asymptomatic, a systolic murmur was identified in the pulmonary area, of progressive intensity, together with an increasing pressure gradient in the region of the pulmonary monocusp. At 2 years of age, it was 25 mmHg; at 5 years, 34 mm Hg; at 7 years, it was 40; at 13 years it was 90 and at 16 years it was 149 mmHg. The patient did not use any specific medications.

Physical Examination: good overall status, eupneic, acyanotic, normal pulses. Weight: 60 Kgs, Height: 165 cm, BP: 110/70 mm Hg, HR: 73 bpm. The aorta was nonpalpable at the suprasternal notch. In the precordium, the apical impulse was nonpalpable and there were no systolic impulses in the left sternal border (LSB). The heart sounds were hyperphonic and a +/+ +/4 rough systolic murmur was auscultated in the pulmonary area and along the LSB. Nonpalpable liver and clear lungs.

Complementary Examinations

Electrocardiogram showed sinus rhythm and signs of complete right bundle-branch block. AQRS = +160°, AP and AT = 50°C. The QRS duration was 0.13". There were no left ventricular potentials, with rR' morphology in V1 and RS in V6.

Chest x-ray showed moderately increased cardiac area on account of the atrial and ventricular arches and normal pulmonary vascular network. Cardiomegaly was progressive since the surgical correction, with a current cardiothoracic index of 0.60 (figure 1).

Keywords

Heart Defects, Congenital; Heart Failure; Truncus Arteriosus/ surgery; Barbero-Marcial Procedure; Diagnostic, Imaging.

Mailing Address: Edmar Atik •

Private office. Rua Dona Adma Jafet, 74, conj.73, Bela Vista. Postal Code 01308-050, São Paulo, SP – Brazil
 E-mail: conatik@incor.usp.br

DOI: <https://doi.org/10.36660/abc.20190490>

Echocardiogram showed a well-positioned interventricular patch and no residual shunt. The right cavities were moderately dilated and showed ventricular dysfunction. The RV also showed hypertrophy. The maximum gradient between the RV and the pulmonary trunk was 149 mmHg, with an average of 86 mmHg. The dimensions were: Ao = 32, LA = 28, RV = 34, LV = 41, septum = posterior wall = 7, LV function = 66%, RPA = 22 and LPA = 26 mm. Mild pulmonary insufficiency.

Cardiac tomography showed normal-sized atria, right ventricle with medio-apical hypertrophy and RVEDV = 135.2 mL/ m² and RV dysfunction = 28%. The RV outflow tract showed a calcified monocusp and the planimetry of the region showed the valve opening was 0.95 cm², with a diameter of 14.3 x 6.2 cm. The interventricular septum was intact, and the aorta had a normal caliber. Measures of interest: 1) Aortic root: 35.4 x 35.0mm (Z-score 3.3). 2) Ascending aorta: 27.6 x 25.2mm. 3) Proximal aortic arch: 22.1 x 20.4mm - mean:



Figure 1 – Chest x-ray highlights the moderate increase in the cardiac area on the account of the right cavities, with normal pulmonary vascular network.

Clinicoradiological Correlation

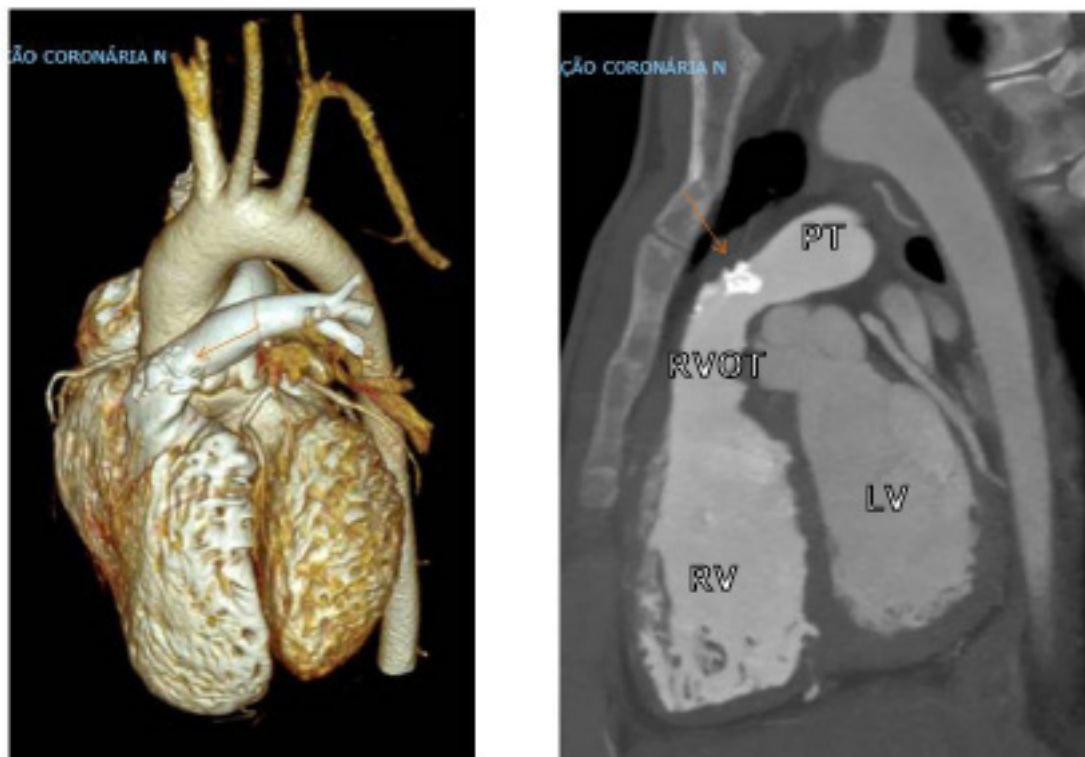


Figure 2 – Angiotomography of the heart in four-cavity and cross-sectional views, highlighting myocardial hypertrophy of the right ventricle and the right ventricular outflow tract without dilation but with a clearly calcified monocusp valve (arrows). Abbreviations: PT: pulmonary trunk, RV: right ventricle, LV: left ventricle, RVOT: right ventricular outflow tract.

23.6 x 17.6mm - distal: 21.0 x 17.6mm 4) Descending aorta: - proximal: 13.9 x 13.5mm - thoraco-abdominal transition: 11.4 x 9.6mm. 5) Pulmonary trunk: 17.1 x 13.6 mm (Z-score -2.27). 6) Right pulmonary artery: 16.3 x 13.0 mm (Z-score 0.35). 7) Left pulmonary artery: 11.7 x 10.1 mm (Z-score -0.96). 9) Left ventricle: - Ejection fraction: 49% - Indexed end-diastolic volume: 82.4 mL / m².

Clinical Diagnosis: *Truncus arteriosus* Type I submitted to an early operation using the Barbero-Marcial technique, with severe and progressive pulmonary stenosis observed in adolescence, in an asymptomatic patient.

Clinical reasoning: The evolution clinical elements were compatible with the diagnosis of progressive pulmonary stenosis since the correction of the basal defect, the *Truncus arteriosus* Type I. The absence of symptoms was expected in the presence of the insidious occurrence of the obstruction over time. The greatest progression of stenosis had occurred in the last three years, probably due to the greater calcification of the monocusp during this period.

Differential diagnosis: Pulmonary valve injury after surgical correction can occur in any situation in which the pulmonary valve is previously repaired. Its diagnosis is simple, attained through the presence of a systolic murmur in the pulmonary area, plus right ventricular myocardial hypertrophy in imaging exams.

Conduct: Considering the progression of the residual defect at the pulmonary valve level, with acquired characteristics such as myocardial hypertrophy and right ventricular dysfunction, the intervention approach in the obstructed region was easily assimilated. Given the adequate anatomy of the pulmonary valve region, with a diameter of 14 mm and without RV outflow tract dilation, it was considered pertinent to approach it using interventional cardiac catheterization. The use of a Melody prosthetic valve was the technique of choice, with the inconvenience of the possibility of occurrence of infectious endocarditis in a bovine jugular vein valve. The fact that the coronary arteries were well away from the right ventricular outflow tract favored the established assumption.

Comments: The use of the Barbero-Marcial¹ technique for correction of the *truncus arteriosus* Type I, developed in 1989, is usually accompanied by pulmonary valve insufficiency due to the RV outflow tract dilation at the anastomosis with the pulmonary trunk, which is pulled towards it. It also accompanies the placement of a monocusp, which, analogously to what occurs after the correction of the Tetralogy of Fallot, also favors the subsequent evolution of progressive pulmonary regurgitation. These patients require correction of the residual defect and almost always by surgical intervention, due to the large dilation in the region, which makes it impossible to place an intravenous prosthesis.

Clinicoradiological Correlation

The preservation of the narrower outflow tract, as observed in the case presented herein, brings to mind the occurrence and discussion of how it should happen in similar operated patients, as most commonly in the Tetralogy of Fallot. This fact could occur more frequently, as long as the surgeon better preserved the RV outflow tract in a narrower area, allowing the pulmonary stenosis evolution to predominate

over valve regurgitation. This preference stems from the fact that the volume overload myocardial lesion is more harmful than pulmonary stenosis, which is caused more often by monocusp calcification.

Ideally, these patients should always be adequately monitored, aiming to preserve the recommended condition for a more favorable evolution in the longer term.

Reference

1. Barbero-Marcial M, Riso A, Atik E, Jatene A. A technique for correction of truncus arteriosus types I and II without extracardiac conduits. *J Thorac Cardiovasc Surg.* 1990;99(2):364-9.



This is an open-access article distributed under the terms of the Creative Commons Attribution License